Measuring copper abundances in the Galactic Bulge

Nikolei Höglinger

Division of Astrophysics
Department of Physics

LUND
UNIVERSITY

2024–EXA220

Degree project of 15 higher education credits
January 2024

Supervisor: Thomas Bensby

Division of Astrophysics
Department of Physics
Box 118
SE-221 00 Lund
Sweden

Abstract

Context: The chemical evolution of Cu in the Galactic bulge have been studied in a few studies using red giant branch stars, but the ages of individual red giant stars are difficult to determine. In addition, the bulge has been a challenging region of the Milky Way galaxy to obtain high-resolution spectra of stars, except when observing through certain few small fields into the bulge that are known to have low extinction. Fortunately, a sample of dwarf and subgiant stars were observed during gravitational microlensing events, whose ages were easily determined for each individual star using isochrone fitting and are widely spread across the longitude of the bottom-half of the Galactic bulge. Previous studies that have analysed the sample of microlensed bulge dwarf stars were successful in measuring the abundances for a variety of elements, but have not made measurements for Cu. Therefore, this work has focused on measuring the abundance of Cu in the Galactic bulge using the sample of microlensed bulge dwarf stars.

Method: The Cu abundances for a sample of 71 microlensed dwarf and subgiant stars that are located in the Galactic bulge were analysed by generating a synthetic spectra with known stellar parameters and fitting it to the observed spectra with the best chosen Cu abundance value for the absorption line at 5782 Å.

Results: The Cu abundances for 31 microlensed bulge stars were reliably measured. It was found that [Cu/Fe] remained flat across metallicities [Fe/H] between $-0.7 \leq$ [Fe/H] ≤ 0.55. Comparing the [Cu/Fe]-[Fe/H] trend of the microlensed bulge stars with that of the Galactic chemical evolution model for the bulge did not agree well with each other, where the bulge model has an relative overproduction of [Cu/Fe] for higher metallicities [Fe/H] > -0.5. The results fit well with the observed [Cu/Fe]-[Fe/H] trend seen in the sample of thick disk dwarf stars for $-0.7 \leq$ [Fe/H] ≤ 0.0 and the ages for the microlensed bulge dwarfs agreed well with the ages of the thick disk dwarf stars. Finally, comparing the Cu abundances with the C and O abundances measured in the microlensed bulge dwarf star sample showed that Cu and C were in lockstep when plotting [Cu/C] vs. [C/H] and it was found that [Cu/O] rises for increasing [O/H] abundances.

Conclusion: From the results, the linear [Cu/Fe]-[Fe/H] trend showed a lockstep behaviour between Cu and Fe, which suggests a dependency between the production of Cu and metallicity. A few microlensed bulge dwarf stars show signs that the formation of the bulge and thick disk are similar. Finally, the rising trend for [Cu/O] for larger [O/H] implies that massive stars, which are believed to be the major producers of Cu, are not the only contributor of Cu and contribution from other sources need to be considered.

Popular Science Summary

Imagine an astronomer meeting an archaeologist in a bar. You might think that they have nothing in common between them. Their fields of study seem very independent from each other. So are their personalities, because one of them is more *down to earth* and keeps getting annoyed at the one who constantly has their *head in the stars*. Puns aside, there is one field of research, in particular, that combines both archaeology and astronomy. This is a field known as *Galactic archaeology*.

Stars are in a continuous cycle of creating and recycling heavy elements. Just like the child possessing the genes of their parents, the next generation of stars capture a portion of the elements that were made and ejected by the previous generation of stars in the local region of the Galaxy. Today, we can see stars in the Galaxy that range in ages between 1 billion to over 12 billion years old, which are as close to the time when the Galaxy was formed. These stars are the fossils for Galactic archaeologists to study how the abundance of a certain element has changed over the lifespan of the Galaxy.

In order to measure the abundance of an element in a star, astronomers need to collect light emitted from the star. More specifically, it is the light that has been absorbed by the elements that allow astronomers to measure its abundance in a star. This requires a good quality spectrum where lots of light is collected from the star. Unfortunately, this is challenging when observing stars in the core of the Milky Way galaxy, which is also known as the Galactic bulge. The solar system is located within the disc of the Galaxy and roughly 26 000 light years from its center. As a result, numerous layers of interstellar dust and gas clouds in the disc obscure our line of sight to the bulge and block the light from the stars. Just like trying to make out the details of something through a thick fog, light from the bulge stars are severely diminished and trying to measure the abundances of elements from faint stars is almost impossible. However, a unique sample of stars were observed during rare events known as *gravitational microlensing events*. Just like how a magnifying glass can start a fire during a sunny day, light from a faint star in the bulge can be magnified toward Earth, causing the brightness of the star to be amplified. During this phenomenon, astronomers can collect more light from a faint star in the bulge and obtain a good quality spectrum to measure the abundances of elements in these stars that were previously hidden deep behind layers of dust and gas in the Galactic bulge.

The goal of this project was to measure the abundance of copper in a sample of microlensed dwarf stars that were observed in the Galactic bulge. This was achieved by generating artificial-programmed spectra with the best copper abundances that best replicate the observed spectra of the stars in the sample. Previous studies have successfully measured the abundances of a variety of elements that commonly measured in stars, such as alpha elements (e.g. oxygen, magnesium). So far, copper has not been measured in the sample of microlensed bulge dwarf stars and has been studied in only a few studies using samples of bulge red-giant stars. Red giants are not good candidates to investigate how

the abundance of copper found in stars have evolved over the lifetime of the Galaxy as the ages of individual red giants are difficult to determine, whereas the ages of individual microlensed dwarf star were easily determined and, thus, makes this an interesting sample to study. This is an opportunity to place copper under the magnifying glass and discover what it can reveal about the Galactic bulge behind its interstellar dusty curtains.

Contents

Chapter 1

Introduction

The Milky Way galaxy is home to a plethora of stars, which were formed at various periods of time during the formation and lifespan of the Galaxy. As a result, stars in the Galaxy today hold a unique composition of elements in their atmosphere that were abundant in the Galaxy at the time of their formation. By localising the stars and measuring the abundances of various elements, the chemical evolution of a specific region of the Galaxy can be investigated. This measurement provides several insights about the formation history of a particular region of the Galaxy. It can reveal the kind of stellar populations (e.g. low-/intermediate-/high-mass stars) that populated the region of the Galaxy at various periods and compare the elemental abundance trend with other regions of the Galaxy to see whether their formation history was similar. In addition to these, the abundance of an element can be compared to another elements, whose production in a star is known, and this can speculate the origins of an element that was previously unknown or uncertain.

The chemical enrichment of elements in the Galaxy is tightly linked to the life cycles of stars. Over the lifespan of the Galaxy, each generation of stars is formed out of gas clouds, which contain various elements that were created by the previous generation of stars and are captured in the atmosphere of the next generation of stars during their formation. Massive stars ($M \geq 10\ M_{\odot}$) progress through several burning stages, building up layers of heavier elements than H and He after each burning stage, until iron (Fe) is formed in their cores. At this stage, no more fusion takes place in the core and the core begins to collapse until it reaches a limit where the nuclear repulsive force between protons and neutrons stops the further collapse of the core (Arcones & Thielemann 2023). This creates a shock wave outwards (Arcones & Thielemann 2023), which will eventually lead to the ejection of the elements that were synthesized during the lifetime of the star. This stage of massive stars is called the core-collapse supernovae (CC SNe), which include SNe type II, Ib and Ic. Low- and intermediate-mass stars ($M < 8\ M_{\odot}$) have a different stellar life cycle than massive stars, where these stars only progress through the H- and He- burning stages that forms a carbon (C) and oxygen (O) core (Arcones & Thielemann 2023). After the He-burning stage, the star begins to pulsate as the He-shell and H-shell surrounding the CO-core ignite and extinguish (Arcones & Thielemann 2023). This pulsation leads to the

star stripping its H- and He- outer layers and leaving behind a CO-core, known as a white dwarf. However, white dwarfs can become reignited if they are in a binary star system with a companion star, where the white dwarf receives a mass transfer from from its companion star (Arcones & Thielemann 2023). In this scenario, the white dwarf will evolve to become an explosive type Ia supernovae (SNe Ia), which is the major contributor of Fe into the Galaxy (Arcones & Thielemann 2023). Through these two types of supernovae, newly-produced elements continuously enrich the interstellar medium (ISM) of the Galaxy and pre-existing elements are captured within the atmospheres of the next generation of stars.

The Galactic bulge is one of three distinct stellar structures that make up the Milky Way galaxy–the other two being the Galactic disc and halo. It is a defining feature for many spiral galaxies, where the bulge is a bright and reddish central core within the disk of galaxies. Many studies have focused to determine whether the bulge and the thin & thick disks of the Milky Way are related, if they both share a similar formation and evolution in the Galaxy.

Unfortunately, obtaining high-resolution spectroscopic data of stars in the Galactic bulge is more challenging than from those that are located in the solar neighborhood. This is because Earth's line of sight towards the bulge is obscured by numerous dense layers of interstellar dust and gas, which severely reduces the brightness of stars in the bulge. As a consequence, studies have relied on analysing the spectra of luminous stars in the red-giant branch and horizontal branch red clump stars (e.g. Zoccali et al. 2006; Fulbright et al. 2007; Lecureur et al. 2007; Johnson et al. 2014; Ernandes et al. 2020) through small windows into the bulge that are known to have low extinction (e.g Baade's window). In addition, red giant stars are an undesirable sample to investigate elemental abundance trends, because the uncertainties in their stellar parameters are larger than for main-sequence dwarf stars and the age of individual stars cannot be easily estimated (Bensby et al. 2017). These are important parameters needed to measure elemental abundances accurately and investigate how the abundances evolved over time in the Galaxy.

However, high-resolution spectra of a unique sample of 91 microlensed dwarf and subgiant stars in the bulge have been obtained by Bensby et al. (2017) in the past decade during several *gravitational microlensing events*. During these events, the brightness of stars are significantly amplified, which allowed the collection of spectra from these faint dwarf stars. Located at the turnoff, the ages of individual dwarf stars were easily determined using isochrone fitting in Bensby et al. (2017), where each isochrone on the Hertzsprung–Russell (HR) diagram is a population of stars with the same age (Kippenhahn et al. 2012). This can be achieved because the isochrones at the turnoff point on the HR diagram are more spread out and distinct isochrones can easily be fitted to stars plotted on the diagram, whereas the isochrones in the red-giant branch are crowded and several isochrones will fit to a star, which makes it very challenging to fit an age to red giant stars using the isochrone fitting method (Bensby et al. 2017). This unique sample of microlensed dwarf stars in the

Galactic bulge provides an opportunity accurately measure the abundance of an element and investigate how it evolved thoughout the lifespan of the Galaxy.

Previous studies (Bensby et al. 2017, 2020, 2021) were able to measure the abundances for a variety of elements in the bulge from the sample of microlensed bulge dwarf stars. Copper (Cu) abundances were measured in only a few studies using red giants and red clump stars (e.g. Johnson et al. 2014; Xu et al. 2019; Ernandes et al. 2020). Therefore, it is an opportunity to provide more Cu abundance measurements for the bulge from the sample of microlensed dwarf stars that provide a timestamp for when they were formed.

Copper is an odd-Z and upper iron-peak element that is part of a group of elements that are slightly heavier than Fe. It is a weak s-process element that is primarily produced during the He-burning stage of massive stars (i.e. Bisterzo et al. 2005; Romano & Matteucci 2007; Pignatari et al. 2010). The s-process is a slow neutron-capture process, where neutrons are captured by iron nuclei until an unstable nucleus decays and releases a beta-minus particle (Arcones & Thielemann 2023). This cycle continues until stable nuclei are reached, which results in the production of elements that are more heavier than Fe. The source of the neutrons comes from the $^{22}\mathrm{Ne}(\alpha,\mathrm{n})^{25}\mathrm{Mg}$[1] reaction, where ^{22}Ne is the product from a double-alpha reaction on ^{14}N during the He-burning stage (Arcones & Thielemann 2023). ^{14}N is the leftover remnant from the H-burning stage that occurred in the core, where a CNO cycle (i.e. CNO-II) is responsible for producing ^{14}N during the H-burning stage (Arcones & Thielemann 2023). Since the CNO cycle is closely related to the production of Cu, Cu is closely depended on the CNO composition (Ishigaki et al. 2013) and the metallicity of the star (Kobayashi et al. 2020).

In this report, Cu abundances were measured from the spectra of microlensed dwarf stars that are located in the bulge. This is done by using a program called PySME to generate a synthetic spectrum with a known Cu abundance input that best fits the observed spectrum of a star. In the next chapter, a more detailed discussion about the microlensed dwarf star sample is presented. Chapter 3 explores the method that was used to measure the Cu abundances in the spectra of the microlensed bulge star sample. The results are presented in Chapter 4 and a discussion about the origins of Cu and comparing the abundance to what was observed in the thick and thin disk is discussed in Chapter 5.

[1]The notation of this reaction means the reaction $^{22}\mathrm{Ne} + \alpha \rightarrow {}^{25}\mathrm{Mg} + \mathrm{n}$.

Chapter 2

The Stellar Sample

This project analysed a total of 71 spectra from the 91 microlensed F- and G-type dwarf, turn-off and subgiant star sample that were previously analysed in Bensby et al. (2017). These stars are a subset of a larger catalogue of microlensed stars that were initially detected by the early warning systems by two photometric, gravitational microlensing surveys that surveyed the Galactic bulge: OGLE (Udalski 2003) and MOA (Bond et al. 2001).

During normal visual observations, the brightness of the stars in the sample are severely diminished to a magnitude of I $\approx$ 18 - 21[1] in the I-band wavelength, because the line of sight towards the Galactic bulge is blocked by several layers of interstellar dust and gas. This would require lengthy exposure times in order to collect high-resolution spectra of each star with sufficiently large signal-to-noise (S/N) ratios[2] (Bensby et al. 2017). During gravitational microlensing events, however, their brightness increase above a magnitude of I $\lesssim$ 15.5, which are opportune moments to collect high-resolution spectra for stars that are in the Galactic bulge. This occurs when a massive object passes between the observer and the star and acts like a magnifying glass that bends the light from the star behind it towards the observer, which results in more photons collected from the star by the telescope and spectrograph. OGLE and MOA regularly observe many fields in the Galactic bulge each year and are able to detect and notify the occurrence of a microlensing event before a star's brightness reaches its peak through their early warning systems.

With the early warning systems from OGLE (Udalski 2003) and MOA (Bond et al. 2001), Bensby et al. (2017) collected high-resolution spectra for a total of 91 microlensed bulge dwarf stars. 71 of the spectra used in this project were collected by the UVES (Dekker et al. 2000) spectrograph's "Red arm", which has a wavelength range of 4200 Å to 11,000 Å, on the ESO's Very Large Telescope on Cerro Paranal near their peak brightness during gravitational microlensing events. As a result, the exposure times to collect these

[1] `https://ogle.astrouw.edu.pl/ogle4/ews/ews.html`

[2] The signal (S) is the number of photons that are collected by the spectrograph of the source (i.e. a star) at certain wavelengths and were converted into electrons on its CCD camera, while the noise (N) is the background photons collected from various background sources.

spectra were significantly reduced to 80 minutes to 2.5 hours. With a 1" and narrower slits, the resolving power UVES was able to achieve in collecting the spectra of the 71 microlensed dwarf sample were between 42,000 and 90,000 and they have a S/N ratio between 15 and 160.

Figure 2.1 shows the Galactic coordinates of the 71 microlensed bulge dwarf stars in the sample. The majority of the stars are found below the Galactic plane of the Milky Way galaxy, with only three stars located above the plane. Stars located below the Galactic plane are well spread across the Galactic longitude between $-6° < l < 7°$, which were achieved through the gravitational microlensing observations. Through this observation method, the microlensed bulge stars can be analysed unrestricted to their position in the bulge, which is an improvement to the sample of stars analysed in previous studies that were observed through small, low-extinction fields into the bulge (e.g Baade's window, Blanco field).

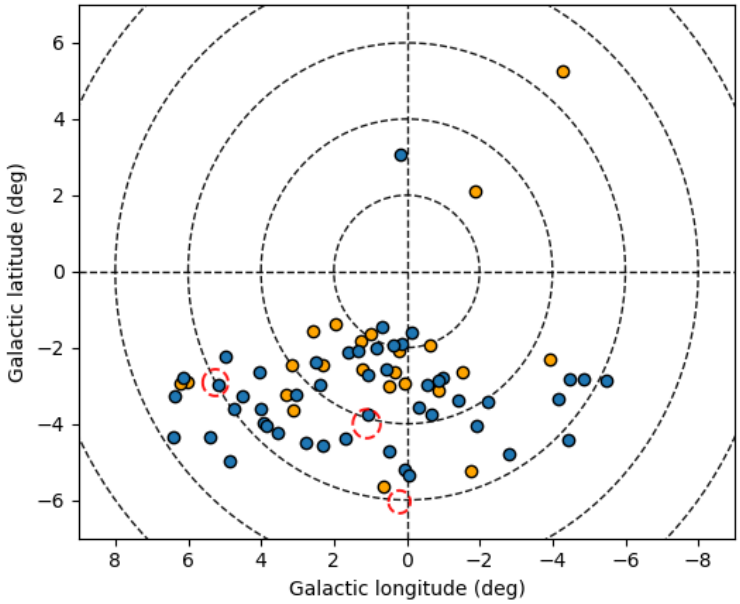

Figure 2.1: The Galactic coordinates of the microlensed star sample in the vicinity of the Galactic center, i.e. (l, b) = (0°, 0°). Blue points indicate the stars whose Cu abundances were able to be measured, while orange points are stars whose Cu abundances were not able to be measured (see Sect. 3.7). The red circular outline indicate the position of three low-extinction fields: Baade's window = (1.14°, −4.2°), two fields at (0.2°, −6°) and (5.2°, −3°). Another field, the Blanco field at (0°, −12°) is not visible in the plot. Their approximate sizes were derived from the positions of the stars in the samples from Xu et al. (2019) and Ernandes et al. (2020).

Stellar parameters (i.e. effective temperature T_{eff}, surface gravity $\log(g)$, microturbulance and metallicity [Fe/H]) for the microlensed star sample were measured by Bensby et al. (2017). In addition, the stellar age for each individual microlensed bulge star in the sample was determined by Bensby et al. (2017).

Lastly, it is useful to confirm whether these microlensed dwarf stars are indeed located in the Galactic bulge. Bensby et al. (2017) confirm the location of the microlensed star sample to be in the bulge. Radial velocities of the microlensed stars measured by Bensby et al. (2017) are consistent with the radial velocities measured in bulge stars and the theoretical depth probabilities calculated in Kane & Sahu (2006) showed that there is a large probability that microlensed stars from all current surveys (e.g OGLE, MOA) are on the far-side of the bulge (Bensby et al. 2017). These conclusions confirm that the microlensed star sample is indeed located within the Galactic bulge.

Chapter 3

Analysis

3.1 Cu I Absorption Line

The abundance of Cu was measured from the absorption line of Cu I at 5782.13 Å. This absorption line is strong enough in almost every spectra of the stellar sample, which makes this line acceptable to use in the measurement of Cu in each microlensed star.

In the close vicinity of the Cu I line, a strong absorption feature was identified in all the spectra in the sample (see Fig. 3.1). This was identified as a diffuse interstellar band (DIB), a unique absorption feature seen in the spectra of stars that appear when observing stars through a region of low density interstellar medium (Geballe 2016). Unlike absorption lines, which are caused by the excitation of molecules inside the star's atmosphere, DIBs are caused by molecules in the interstellar gas clouds within the Galactic disk that obscure the line of sight towards the bulge and are commonly spotted in the spectra of reddened stars (Geballe 2016). This particular DIB was identified at 5780 Å from Jenniskens & Desert (1994) and it aligns well in all the spectra in the sample where the continuum of the spectra dips down over a few wavelength. This is, therefore, definitely a DIB in all the spectra. Due to the spectra having been wavelength shifted to account for the stars' various radial velocities, the position of the 5780 Å DIB varies slightly for each spectra, which results in the Cu I absorption line to be often located within the DIB, in the wing or outside the DIB. It is therefore important to remove this DIB in the analysis of the spectra before making a Cu abundance measurement of the absorption line.

3.2 PySME

In order to measure the abundance of Cu from the absorption line, a python implementation of SME (Spectroscopy Made Easy) called PySME was used, which generates a synthetic spectrum with known stellar parameter of a star and fits the observed spectrum of the star. With the synthetic spectrum, the abundance of Cu can be freely altered, which in

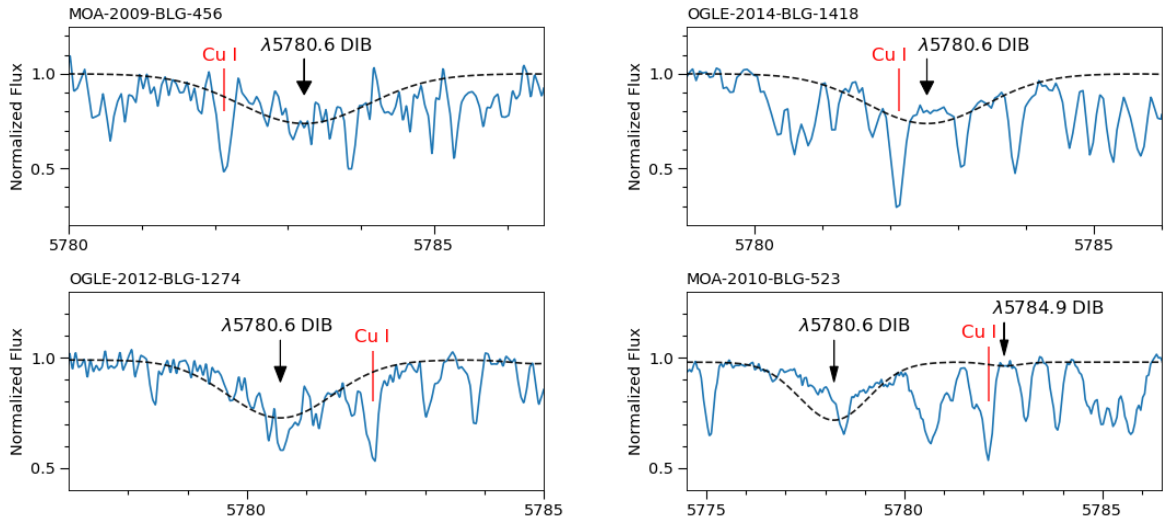

Figure 3.1: The red line indicates the absorption line of Cu I at 5782 Å and shows how the different radial velocities, which have been accounted for the wavelength shift, in the stars move the position of the DIB(s). The profile of the DIBs illustrated in the figures were generated using the procedure in Jenniskens & Desert (1994) (`https://leonid.arc.nasa.gov/DIBcatalog.html`).

turn changes the absorption line at 5782 Å in the synthetic spectrum and is used to find the best Cu abundance value that fits the absorption line in the observed spectrum of a star.

PySME requires several inputs in order to generate a synthetic spectrum for the observed spectrum of a star in the sample. The stellar parameters (i.e. effective temperature T_{eff}, surface gravity log(g), metallicity [Fe/H] and microturbulance ξ) specific for the star. Other inputs required is a linelist, which identifies the wavelength of the elements in the wavelength range of the star's spectrum and their line properties (e.g. energy states, statistical weight, oscillator strength), and a stellar model atmosphere, which is a theoretical model of the atmosphere of a star. The linelist was acquired from the VALD database and a MARCS stellar atmosphere model was used. Since there were no NLTE grid models for Cu, a MARCS 2012 model was used instead with the assumption of a local thermal equilibrium (LTE) for the stellar atmosphere.

3.3 Spectra Analysis

3.3.1 Normalizing the Spectra

Before the Cu abundance from a star's spectrum was measured, the observed spectrum needed to be normalized first, such that the synthetically-generated spectra from PySME

fits the observed spectrum properly. This was achieved by fitting a continuum function to the observed spectra.

First, several wavelength regions in the vicinity of the Cu absorption line were highlighted, as seen in Fig. 3.2(a). These regions lie on the continuum. A function that is generated to normalize the spectrum must pass through each of these highlighted regions in order to properly normalize the spectra and fit the synthetic spectra generated for each observed spectra.

With each highlighted wavelength regions, data points were generated within these regions and a spline function was generated to fit through these points, as seen in Fig. 3.2(a). For those spectra with low S/N ratios, data points were generated through the middle of a noisy spectrum, so that the spline function passes though the middle of the noise. Through this method, a continuum of the spectra is plotted by the spline functions and the DIB, which affects this region of the spectrum and the Cu absorption line, is removed. The spectra were then normalized using the spline functions fitted and the resulting normalized spectra are fitted with the synthetic spectra generated by PySME, as seen in Fig. 3.2(b).

3.3.2 Measuring the Cu Abundance

Once the observed spectra were normalized and each normalized spectra were fitted with their synthetic spectra, the Cu abundances were measured. Ten synthetic spectra were generated with slightly varying Cu abundance values (see Fig. 3.2(b)). A χ^2-minimisation procedure was performed by taking the sum of the squared differences between the observed spectrum and ten synthetic spectra at each wavelength within the Cu absorption line, which lie within the pair of black vertical lines in Fig. 3.2(b). The best fitting synthetic spectrum to the normalized spectrum will have the lowest χ^2 value and the Cu abundance at the minimum χ^2 value was taken as the absolute Cu abundance[1] for the star.

3.4 Calculating Abundance Ratios

To compare the Cu abundances measured with the abundance of a different element, an abundance ratio [Cu/X] (where X is any element, e.g. Fe, O) is calculated for each microlensed star in the sample[2]. This abundance ratio is relative to the solar ratio.

[1] The absolute abundance ϵ(Cu) is equal to $\epsilon(\mathrm{Cu}) = \log(\mathrm{N_{Cu}/N_H}) + 12$, where $\log(\mathrm{N_{Cu}/N_H})$ is the ratio between the number of Cu and H atoms and H is taken as the reference abundance.

[2] i.e. $[\mathrm{Cu/X}] = [\mathrm{Cu/X}]_{\mathrm{star}} - [\mathrm{Cu/X}]_{\odot} = \log(\mathrm{Cu/X})_{\mathrm{star}} - \log(\mathrm{Cu/X})_{\odot}$.

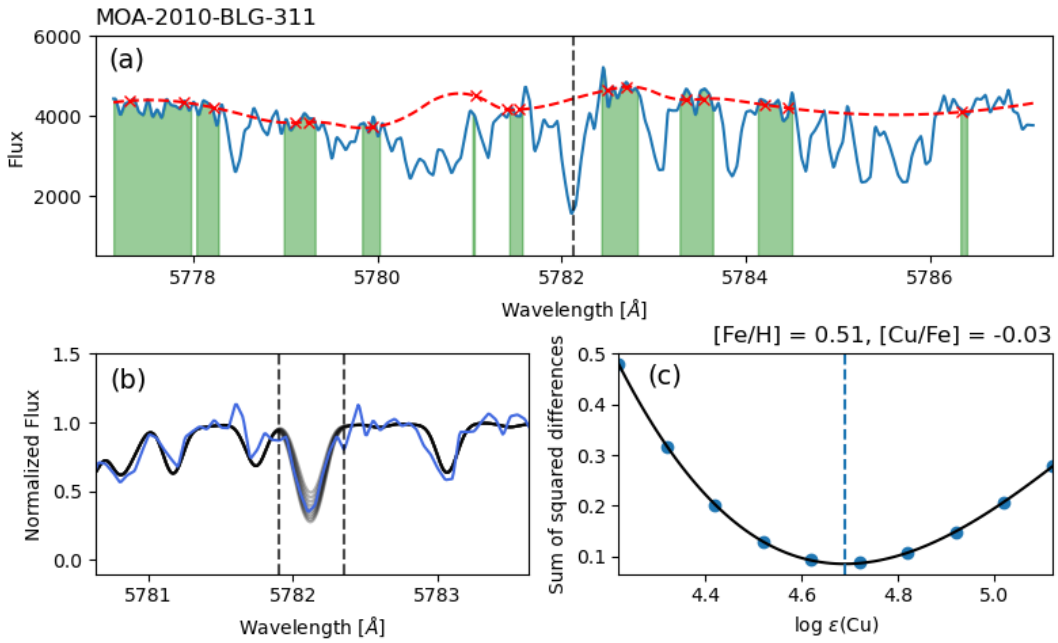

Figure 3.2: (a) The continuum function fit using a spline function. The black-dashed line indicate the absorption line of Cu at 5872 Å. (b) The normalized observed spectrum of a sample star MOA-2010-BLG-311 and the synthetic spectra generated. The two dashed lines indicates the range where the χ^2-minimisation had been applied to. (c) The sum of the squared differences between the observed and synthetic spectra. The blue dashed line indicates the lowest χ^2 value at which the Cu abundance is chosen for the spectral line.

3.5 Uncertainty Analysis

All four stellar parameters (i.e. T_{eff}, log(g), [Fe/H] and ξ) used to measure the Cu abundance from the spectra have uncertainties that need to be taken into account as an uncertainty for the Cu abundance. Their uncertainties were taken from Bensby et al. (2017). Without changing the procedure of obtaining the Cu abundance, four Cu abundances were measured by changing each stellar parameter individually to its upper limit[3]. The difference between the four abundance values and the original Cu abundance measurement for the spectrum were calculated. and the uncertainties on the Cu abundance when considering the uncertainties for each stellar parameters individually were obtained. All four calculated differences are then used in a standard deviation calculation,

$$\sigma = \sqrt{\sigma_{teff} + \sigma_{logg} + \sigma_{[Fe/H]} + \sigma_{\xi}}, \tag{3.1}$$

which will give the uncertainty for the Cu abundance measured for the absorption line in a star's spectrum. This final uncertainty will, thus, include all the Cu abundances that are

[3]In other words, the first Cu abundance was measured with (T_{eff}+Δ_{teff}, log(g), [Fe/H], ξ), the second Cu abundance was measured with (T_{eff}, log(g)+Δ_{logg}, [Fe/H], ξ), etc.

calculated in the uncertainty of each stellar parameters.

3.6 Deviating Spectrum Analysis

For one star, OGLE-2014-BLG-0801, it needed a slight adjustment to one parameter in its analysis. Its log(g) value ($\log(g) = 2.9 \pm 0.28$) was too low for the model atmosphere (i.e. a minimum of $\log(g) = 3.0$), which results in an error in generating the synthetic spectra for this particular star. To fix this error and allow the analysis of this star's spectrum, the star's log(g) value was changed to 3.0. Although this change does affect the final Cu abundance measured for the star, the change would be small and the changed log(g) value falls within the uncertainty of the original log(g) value, which will result in the uncertainty of the new abundance to include the abundances that would be using the original log(g) value.

3.7 Removed Spectra

After the analysis procedure for the 71 microlensed bulge star spectra, there were 23 spectra that could not be used to measure their Cu abundance. These spectra can be seen in the appendix: A.3.

Chapter 4

Results

4.1 Abundance trend of Cu

Fig. 4.1 shows the measured Cu abundance ratio [Cu/Fe] with respect to the metallicities [Fe/H] and ages for the analysed microlensed bulge stars in the sample. The [Cu/Fe]-[Fe/H] trend remains constant across metallicities between $-0.7 \lesssim$ [Fe/H] $\lesssim 0.55$ and lies slightly above the solar [Cu/Fe] ratio at [Cu/Fe] = 0.04. In terms of the ages of the stars, there is a smooth transition, where the metallicity increases in more younger bulge stars. This result implies that the abundance of Cu is in lockstep with the abundance of Fe. The abundance of Cu has also increased over time, because the constant [Cu/Fe] ratio shows that old low-metallicity stars have a lower Cu abundance than younger higher-metallicity stars.

4.2 Outliers & Noisy Spectra

Out of the 48 star spectra where Cu abundances were measured, 17 results are highlighted in Fig. 4.2 that were noted to have flux peaks within the Cu absorption line which distort the shape of the line (see appendix A.2). Due to the way the Cu abundance is measured, the flux peaks are affecting the chosen Cu abundance value in the analysis of these spectra, which either lowers or raises the χ^2 values of an individual synthetic spectrum during the analysis and this has shifted the minimum where the final Cu abundance was determined away from the true Cu abundance.

A likely cause for these flux peak occurrences might be the low S/N ratio of the spectra, because the majority of 17 spectra that were noted to have flux peaks within their spectral line have a S/N ratio of 25.0, 30.0, and 35.0. However, for a couple of spectra (i.e. MOA-2010-BLG-049, OGLE-2012-BLG-1274), the maximum S/N ratio were unusually high at 90.0. At this S/N ratio, the spectra should very few to none of these flux peaks, because the majority of the "good" spectra (i.e. not highlighted in the plot) have

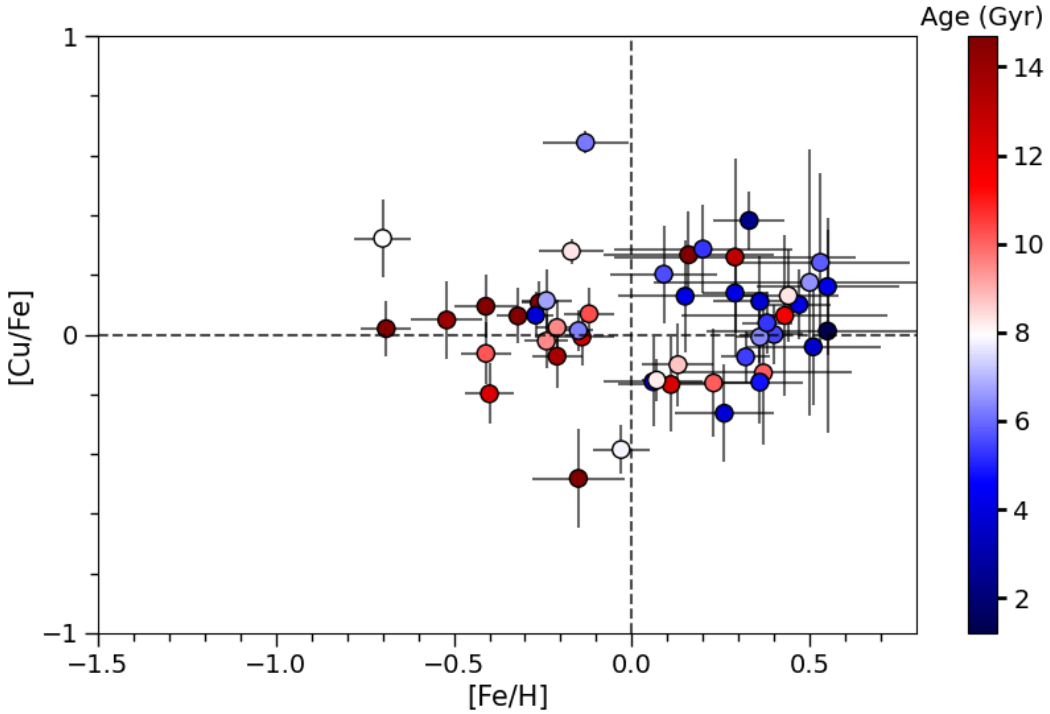

Figure 4.1: [Cu/Fe] against the metallicity [Fe/H] of the microlensed bulge stars in the sample along with their error bars. The results are colour-coded based on their ages.

a S/N ratio of 45.0, 50.0 and 55.0. An argument against this is a few good spectra (i.e. MOA-2012-BLG-391, MOA-2013-BLG-402, MOA-2014-BLG-131, OGLE-2012-BLG-1526, OGLE-2015-BLG-0159) that have the minimum S/N ratio of 25.0 and 35.0, which is as low as the highlighted spectra, but are not as severely disrupted by flux peaks. These spectra also have the possibility to being placed into the highlighted group of spectra, even if the flux peaks are not as severe. It is likely that the low S/N ratio in spectra are causing these flux peaks to appear within the Cu spectral line.

One spectrum, OGLE-2014-BLG-0953 (top right in Fig. A.9), had an unusually deep Cu absorption line, where the synthetic spectrum with a higher chosen Cu abundance value cannot properly fit the observed spectral line, because it reaches its saturation point before it can fit the observed line. This suggests that the spectral line is being diminished and causing the Cu abundance to be much higher than what is determined.

Since the Cu abundance of these spectra are highlighted as being uncertain, the following discussion about the Cu abundance results will excluded these abundances. Removing these abundance does not change the overall trend as it was described in Sect. 4.1.

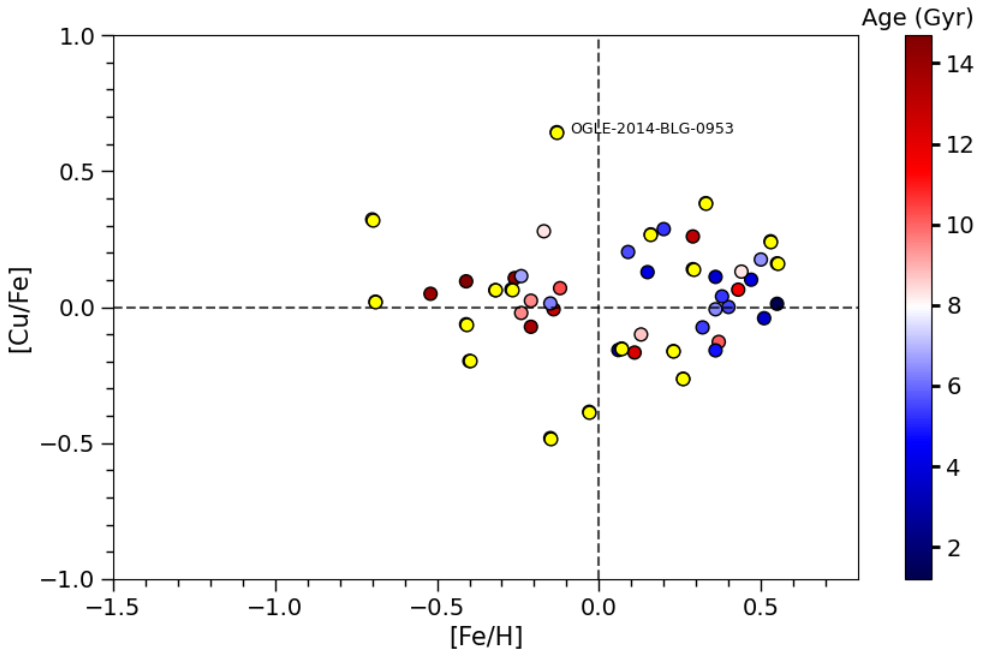

Figure 4.2: [Cu/Fe] vs. [Fe/H] results similar to Fig. 4.1, but those Cu abundances that are noted as uncertain are highlighted yellow. The named data point is indicated as an outlier to the abundance trend.

4.3 Comparisons with Previous Studies

Fig. 4.3 shows the comparison with the results from two red giant star samples studied in Xu et al. (2019) (solid grey triangles) and Ernandes et al. (2020) (grey crosses). Uncertain Cu abundances that were highlighted in Fig. 4.2 were removed. The flat [Cu/Fe]-[Fe/H] trend for the microlensed bulge stars is consistent to that of the trends from the red giants for [Fe/H] $\gtrsim -0.7$. There are no microlensed bulge stars in the present work with metallicities [Fe/H] $\lesssim -0.7$ to show whether the [Cu/Fe]-[Fe/H] trend declines with decreasing metallicity as it is seen in results for the red giant stars. For all the microlensed dwarf stars, they were formed after a bend in the trend.

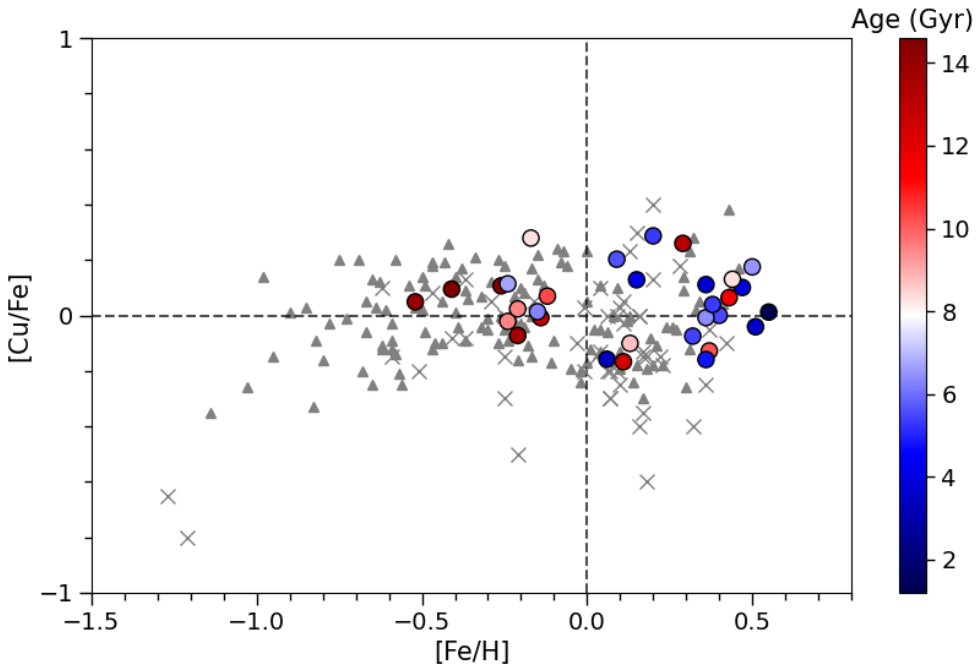

Figure 4.3: [Cu/Fe]-[Fe/H] trend comparison between the microlensed bulge dwarf star sample and sample of red giants and red clump stars from Xu et al. (2019) (*solid grey triangles*) and Ernandes et al. (2020) (*grey crosses*). Results for the microlensed bulge stars are colour-coded based on their age.

Chapter 5

Discussion

5.1 Comparisons with Galactic Chemical Evolution models

In Fig. 5.1(a), several Galactic chemical evolution (GCE) models for Cu are plotted over the [Cu/Fe]-[Fe/H] results from the microlensed bulge stars. The models included are for the bulge (red dashed line), the thick disk (blue dashed line) and the solar neighborhood (green dashed line) taken from Kobayashi et al. (2011) and Kobayashi et al. (2020). These models are calculations for the evolution of the [Cu/Fe]-[Fe/H] in the region of the Galaxy, which consider the stellar yields from various sources (e.g. core-collapse SNe, SNe Ia, AGB star) and set various parameters unique to bulge, thick disk and solar neighborhood, e.g. their formation history, initial conditions and gas flow (Matteucci 2016), to fit best the observed data Kobayashi et al. (2011, 2020) were using.

The bulge model was set to have a fast star formation period in the first 3 Gyr of the Galaxy, which reaches solar metallicity ([Fe/H] = 0) after 1 Gyr (Kobayashi et al. 2020). Massive stars rapidly raise the metallicity in the early bulge, because they are shorter-lived than low- & intermediate-mass stars. As a result, [Fe/H] rises rapidly and the production of Cu rises as well because of its dependency to the metallicity of the star (Kobayashi et al. 2011). The bend in the [Cu/Fe]-[Fe/H] only occurs after significantly large metallicity low- and intermediate-mass stars contribute to the enrichment through SNe Ia.

The bulge model, however, appears to have an overproduction of Cu after [Fe/H] $\gtrsim -0.7$ than what is observed for the microlensed bulge stars. The Cu enrichment model for the thick disk from Kobayashi et al. (2011) (blue dashed line) is also slightly overproduced. The thick disk model was set with a rapid star formation period as fast as the bulge model (3 Gyr), but set with a smaller star formation efficiency[1] than in the bulge model (Kobayashi et al. 2020). Since both of these of models have an overproduction of Cu compared to the

[1]The star formation efficiency measures the efficiency of the interstellar gas to form stars (Leroy et al. 2008).

trend from the microlensed bulge stars, it suggests that the the star formation period of the early bulge might not be as rapid as it is believed to be in the models by Kobayashi et al. (2011, 2020). The recent model for the solar neighborhood from Kobayashi et al. (2020) (green dashed line) has an underproduction of Cu than what is observed for the microlensed bulge stars. It is modeled with a slower star formation and lower star formation efficiency than in the bulge and thick disk model (Kobayashi et al. 2020).

What the models and the observed trend, however, both agree is the behaviour of the trends after the SNe Ia begin to contribute. In all the models, SNe Ia occur after [Fe/H] ≈ -1 (Kobayashi et al. 2011), which enrich the ISM with Fe. As a result, all the models show a constant [Cu/Fe]-[Fe/H] trend after the bend, because low- and intermediate-mass are also producing Cu (Kobayashi et al. 2011). This behaviour in the [Cu/Fe]-[Fe/H] trend agrees well with what is observed for the microlensed bulge stars, which suggests that Cu is being produced in the progenitor low-/intermediate-mass star.

5.2 Comparisons with Disk stars

Reddy et al. (2003, 2006) measured the [Cu/Fe] abundance in F- and G-type dwarf stars in the thin & thick disk with metallicities [Fe/H] ≥ -1.6. The [Cu/Fe] abundance for the microlensed bulge stars are plotted together with the results from Reddy et al. (2003, 2006) in Fig. 5.1(b).

Little data is available for thin & thick disk stars with metallicities greater than the solar metallicity [Fe/H] ≥ 0.0. Reddy et al. (2003, 2006) results contain a similar bend in the [Cu/Fe] trend at [Fe/H] ≈ -0.8 as it was seen in the samples of red giant stars in Fig. 4.3. For $-0.7 \leq$ [Fe/H] ≤ 0.0, many of the microlensed bulge stars fit well with the thick-disk [Cu/Fe] trend, which show an enhanced [Cu/Fe] abundance ratio more than in the thin-disk stars. There are a few microlensed bulge stars that fit the [Cu/Fe] trend for the thin-disk stars. The stellar ages of the thick- and thin-disk stars also agree well with the ages of the microlensed bulge stars, where thick-disk stars after [Fe/H] ≥ -0.7 are around 12 Gyr and around 6 Gyr at [Fe/H] $= 0.0$ (Reddy et al. 2006), and the thin-disk stars have an upper bound age of about 10 Gyr at [Fe/H] ≈ -0.7 (Reddy et al. 2003). Finding these two distinct branches in the [Cu/Fe] trend for disk star that fit well with the microlensed bulge stars at metallicities $-0.7 \leq$ [Fe/H] ≤ 0.0 shows hints that the bulge is closely related to the formations and evolution of the thick- and thin-disk of the Galaxy.

5.3 Comparisons with C and O

Fig. 5.2 shows the Cu abundances for the microlensed star sample compared with three elements as reference elements: carbon (C) and oxygen (O), which were both measured in Bensby et al. (2021) for the microlensed bulge star sample. Carbon is used here to

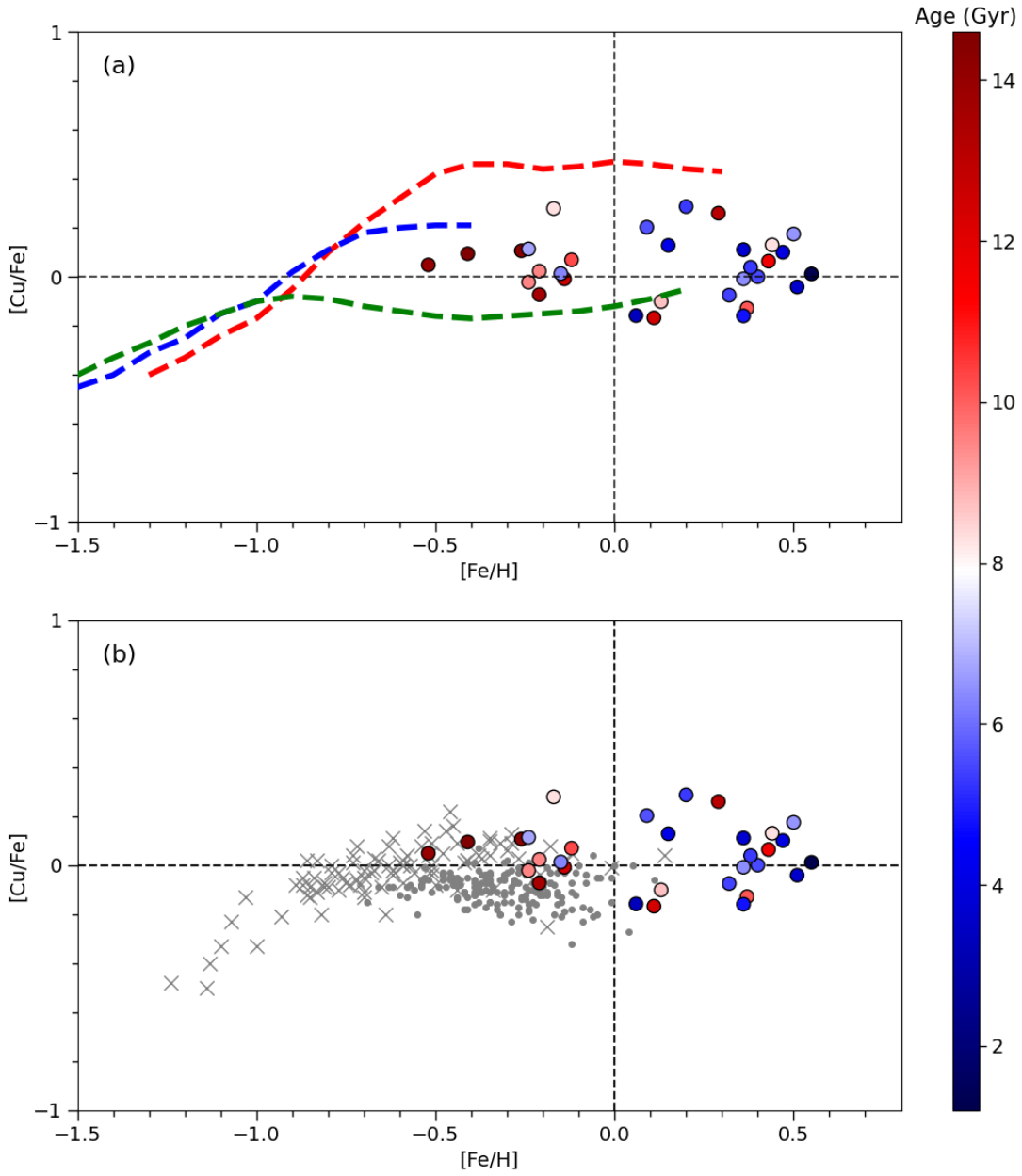

Figure 5.1: (a) GCE models for Cu in the bulge (*red dashed line*) from Kobayashi et al. (2011), in thick disk (*blue dashed line*) from Kobayashi et al. (2011) and the solar neighborhood (*green dashed line*) from Kobayashi et al. (2020) plotted over the results from the microlensed bulge star sample. (b) Comparison between the [Cu/Fe]-[Fe/H] trend for the thick-disk dwarf stars (*grey crosses*) from Reddy et al. (2006), the thin-disk dwarf stars (*solid grey circles*) from Reddy et al. (2003) and the microlensed bulge dwarfs. Microlensed bulge stars are colour-coded according to their ages.

investigate whether the Cu production is dependent on the initial composition of the CNO cycle (Ishigaki et al. 2013), which is also closely dependent on the metallicity. Oxygen is commonly used as an indicator to see whether an element is produced in massive stars, because the major producer of oxygen is well known to be massive stars (e.g. Woosley & Weaver 1995).

The [Cu/C]-[C/H] trend in Fig. 5.2(b) remains constant as the abundance of C increases, which is similar to the trend with Fe that is seen for [Cu/Fe] vs. [Fe/H]. Cu increases in lockstep with C, as it also did with Fe, which implies that the production of Cu directly linked to the carbon composition in the CNO cycle reactions during the H-burning stage and is dependent on the metallicity of the progenitor star.

The [Cu/O]-[O/H] trend in Fig. 5.2(c) shows a rapid rise in the [Cu/O] ratio, which suggest that the production of Cu increases while O is produced in massive stars. The stars in the sample were formed after the time delay between SNe II and SNe Ia contributions, hence the increase in [Cu/O] happens during the time when low- and intermediate-mass star contribute to the enrichment of the ISM alongside the enrichment from massive stars. If massive stars produced the majority of Cu, the [Cu/O] would most likely have remained constant, but this rapid increase of Cu suggests that other sources of Cu are non-negligible. This behaviour is very similar to the [C/O]-[O/H] trend seen in Bensby et al. (2021) (Fig. 8) using the same microlensed bulge star, where the trend also experiences the same increase for larger metallicities.

5.4 A potential source of systematic error

There is a potential systematic error within the Cu abundances measured for each spectrum, where the placement of the continuum could result in a different Cu abundance measurement. For each star spectrum in the sample, their continuum were determined very carefully in order to measure an accurate Cu abundance, which is evident by the good fits between the synthetic generated spectra and normalized observed spectra after determining their continuum. Spectra with high S/N ratios were easier to analyse and determine their continuum, however for those spectra that have a low S/N, the placement of the continuum could slightly higher or lower at some points, which would impact the Cu abundance measured. It was the decision to place the continuum for the spectra so that the synthetic spectra generated from PySME would pass through the middle of a noisy region of the observed spectrum.

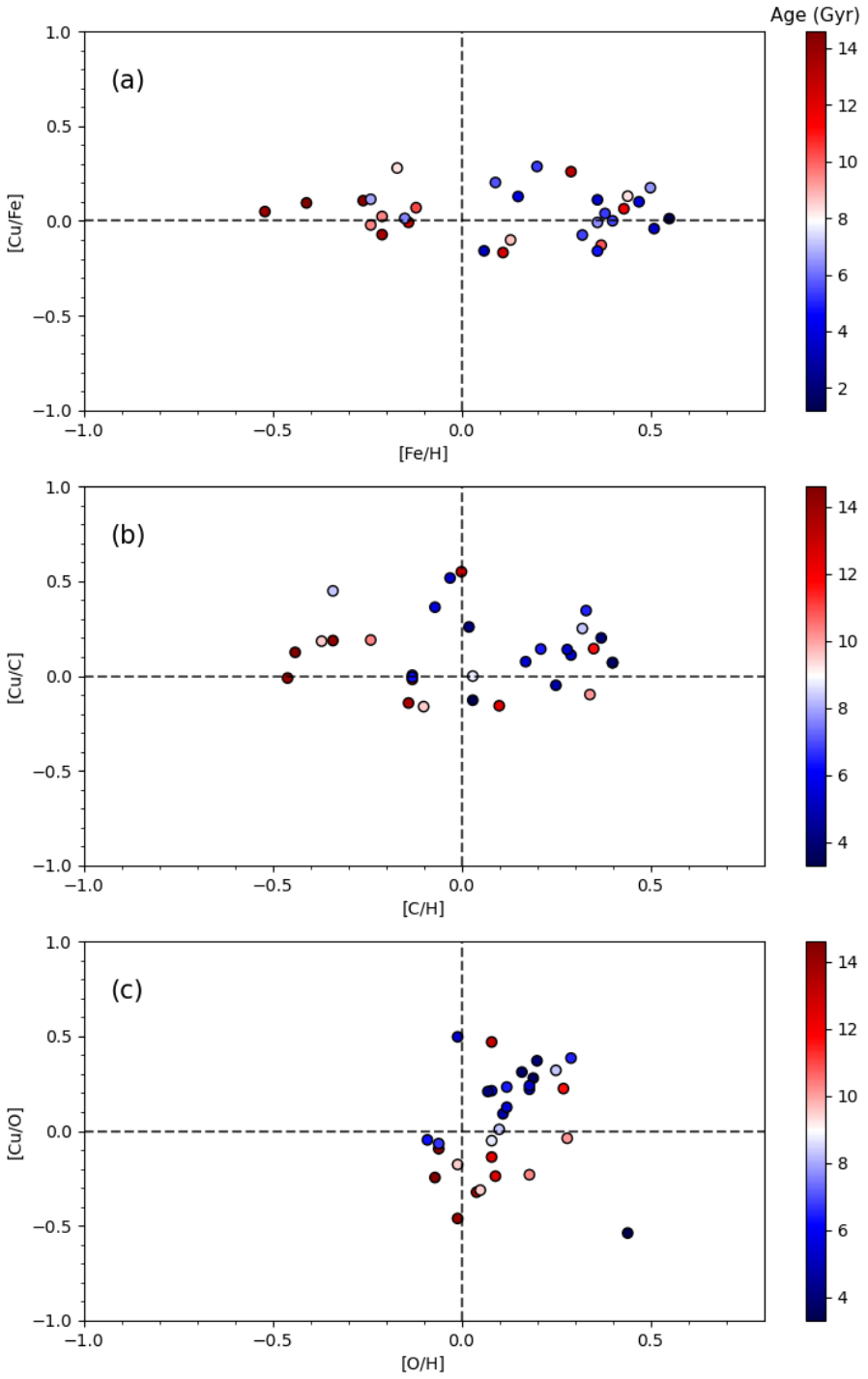

Figure 5.2: (a) [Cu/Fe] vs. [Fe/H], (b) [Cu/C] vs. [C/H] and (c) [Cu/O] vs. [O/H] for the microlensed bulge dwarf star sample.

Chapter 6

Conclusions

The abundance of Cu were measured in 48 microlensed dwarfs and subgiants that are in the Galactic bulge. Synthetic spectra were generated using PySME with a chosen Cu abundance that best fits the absorption line at 5782 Å in the observed spectra of the microlensed stars. The [Cu/Fe] abundance ratios were then determined and plotted against the metallicity [Fe/H] of the microlensed stars, as well as [Cu/C]-[C/H] and [Cu/O]-[O/H] plots were made. The findings from this work can be summarised in the following points:

- The [Cu/Fe]-[Fe/H] abundance trend showed a constant [Cu/Fe] trend between metallicities $-0.7 \leq$ [Fe/H] ≤ 0.55. This shows that Cu is in lockstep with Fe as the metallicity increases.

- The flat [Cu/Fe]-[Fe/H] abundance trend for the microlensed bulge dwarf stars between $-0.7 \leq$ [Fe/H] ≤ 0.55 is consistent with the trend seen for samples of red giants from Xu et al. (2019) and Ernandes et al. (2020).

- Galactic chemical evolution model from Kobayashi et al. (2011) for the Galactic bulge showed an overproduction of [Cu/Fe] which did not agree with the [Cu/Fe] ratio seen for the microlensed bulge stars.

- The [Cu/Fe]-[Fe/H] trend seen from the microlensed bulge stars follow the trend seen in the Galactic thick disk between metallicities $-0.7 \leq$ [Fe/H] ≤ 0.0 and the ages of the bulge stars followed the range of ages for the thick disk stars in the metallicity region.

- From the [Cu/C]-[C/H] abundance trend, Cu and C are in lockstep in the Galactic bulge. This suggests that the production of Cu is dependent on the C composition of the CNO cycle during the H-burning stage of stars, which also shows the Cu production is dependent on the metallicity of the star. To determine whether Cu originates in massive stars, the [Cu/O]-[O/H] trend showed a rising [Cu/O] trend towards higher [O/H]. This suggests that massive stars are not the major producer of Cu and other sources, potentially SNe Ia, are non-negligible.

Acknowledgements

I am very grateful to my supervisor, Thomas Bensby, for providing me with continuous support thoughout four months of the project and his guidance whenever I encountered writer's block. Many thanks to my family, friends and teachers who have given me immense support and valuable experiences thoughout my life.

Bibliography

Arcones, A. & Thielemann, F. K. 2023, The Astronomy and Astrophysics Review, 31, 1

Bensby, T., Feltzing, S., Gould, A., et al. 2017, A&A, 605, A89

Bensby, T., Feltzing, S., Yee, J. C., et al. 2020, A&A, 634, A130

Bensby, T., Gould, A., Asplund, M., et al. 2021, A&A, 655, A117

Bisterzo, S., Pompeia, L., Gallino, R., et al. 2005, Nuclear Physics A, 758, 284

Bond, I. A., Abe, F., Dodd, R. J., et al. 2001, MNRAS, 327, 868

Dekker, H., D'Odorico, S., Kaufer, A., Delabre, B., & Kotzlowski, H. 2000, in Society of Photo-Optical Instrumentation Engineers (SPIE) Conference Series, Vol. 4008, Optical and IR Telescope Instrumentation and Detectors, ed. M. Iye & A. F. Moorwood, 534–545

Ernandes, H., Barbuy, B., Friaça, A. C. S., et al. 2020, A&A, 640, A89

Fulbright, J. P., McWilliam, A., & Rich, R. M. 2007, ApJ, 661, 1152

Geballe, T. R. 2016, in Journal of Physics Conference Series, Vol. 728, Journal of Physics Conference Series, 062005

Ishigaki, M. N., Aoki, W., & Chiba, M. 2013, ApJ, 771, 67

Jenniskens, P. & Desert, F. X. 1994, A&AS, 106, 39

Johnson, C. I., Rich, R. M., Kobayashi, C., Kunder, A., & Koch, A. 2014, AJ, 148, 67

Kane, S. R. & Sahu, K. C. 2006, ApJ, 637, 752

Kippenhahn, R., Weigert, A., & Weiss, A. 2012, Stellar Structure and Evolution, 2nd edn., Astronomy and Astrophysics Library (Springer Berlin, Heidelberg)

Kobayashi, C., Karakas, A. I., & Lugaro, M. 2020, ApJ, 900, 179

Kobayashi, C., Karakas, A. I., & Umeda, H. 2011, MNRAS, 414, 3231

Lecureur, A., Hill, V., Zoccali, M., et al. 2007, A&A, 465, 799

Leroy, A. K., Walter, F., Brinks, E., et al. 2008, AJ, 136, 2782

Matteucci, F. 2016, in Journal of Physics Conference Series, Vol. 703, Journal of Physics Conference Series, 012004

Pignatari, M., Gallino, R., Heil, M., et al. 2010, ApJ, 710, 1557

Reddy, B. E., Lambert, D. L., & Prieto, C. A. 2006, Monthly Notices of the Royal Astronomical Society, 367, 1329

Reddy, B. E., Tomkin, J., Lambert, D. L., & Prieto, C. A. 2003, Monthly Notices of the Royal Astronomical Society, 340, 304

Romano, D. & Matteucci, F. 2007, MNRAS, 378, L59

Udalski, A. 2003, Acta Astronomica, 53, 291

Woosley, S. E. & Weaver, T. A. 1995, ApJ, 101, 181

Xu, X. D., Shi, J. R., & Yan, H. L. 2019, ApJ, 875, 142

Zoccali, M., Lecureur, A., Barbuy, B., et al. 2006, A&A, 457, L1

Appendix A

Collection of Spectra in the Sample

A.1 Spectra in the final results

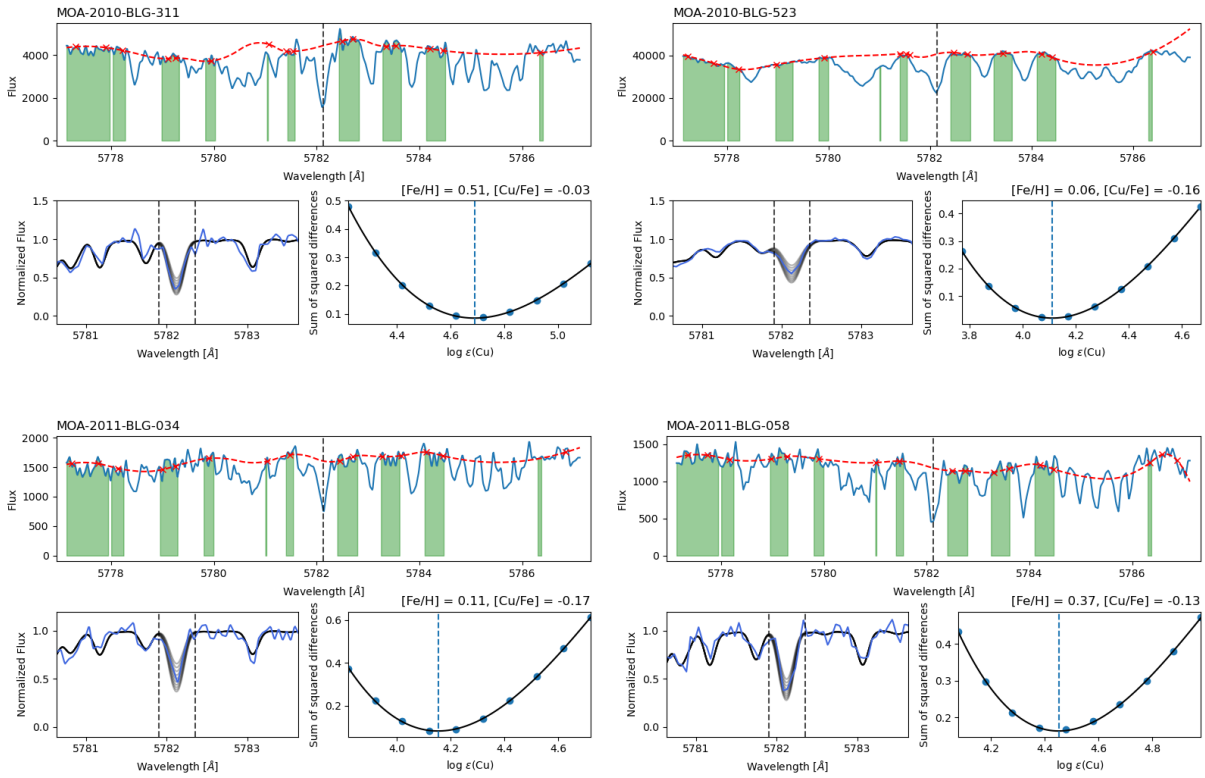

Figure A.1: Spectra of the microlensed bulge dwarf star sample that have been analysed and measured Cu abundance fro the Cu spectral line at 5782 Å. These results are shown in the plots in Ch. 5.

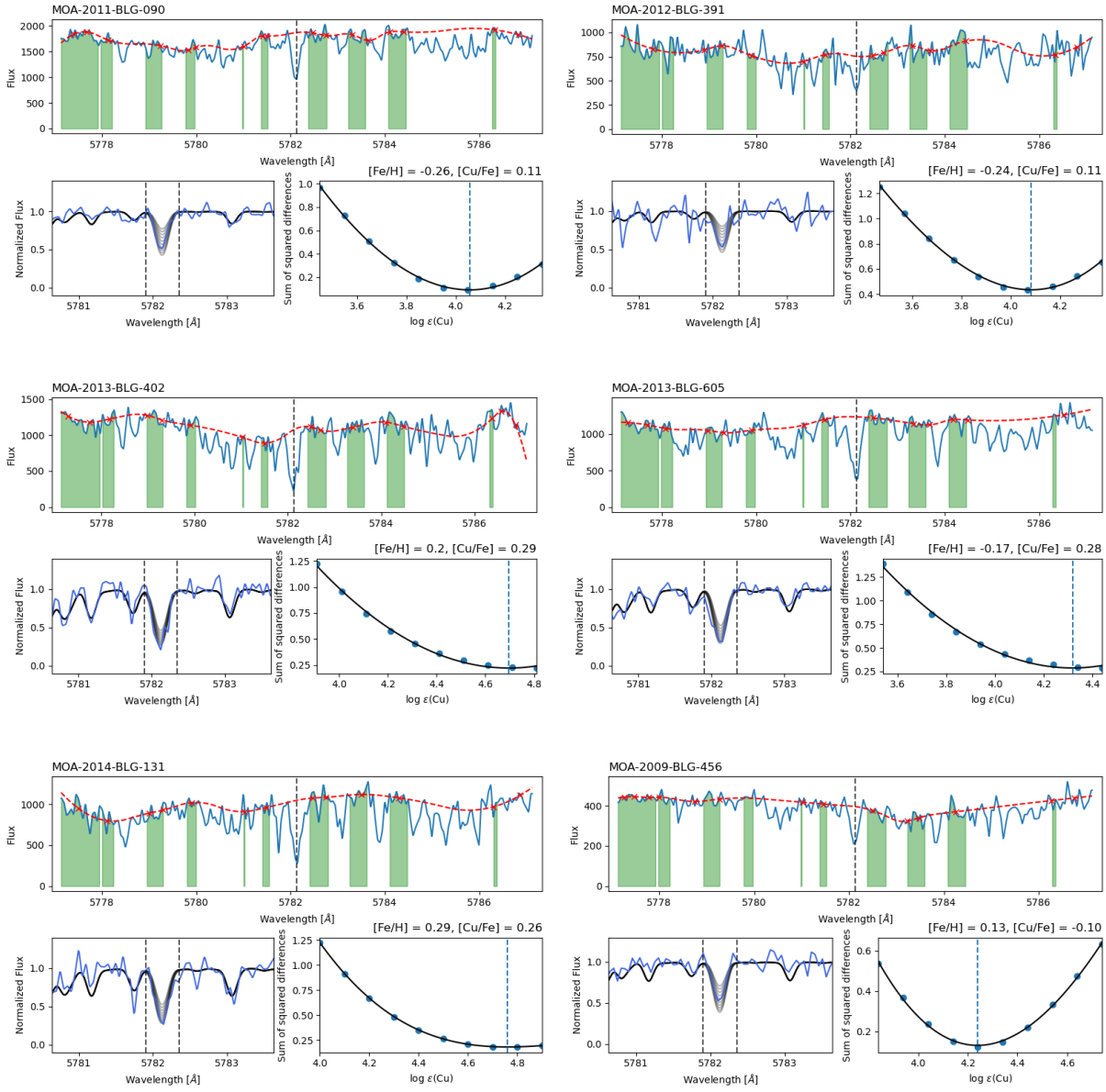

Figure A.2: Same as in Fig. A.1.

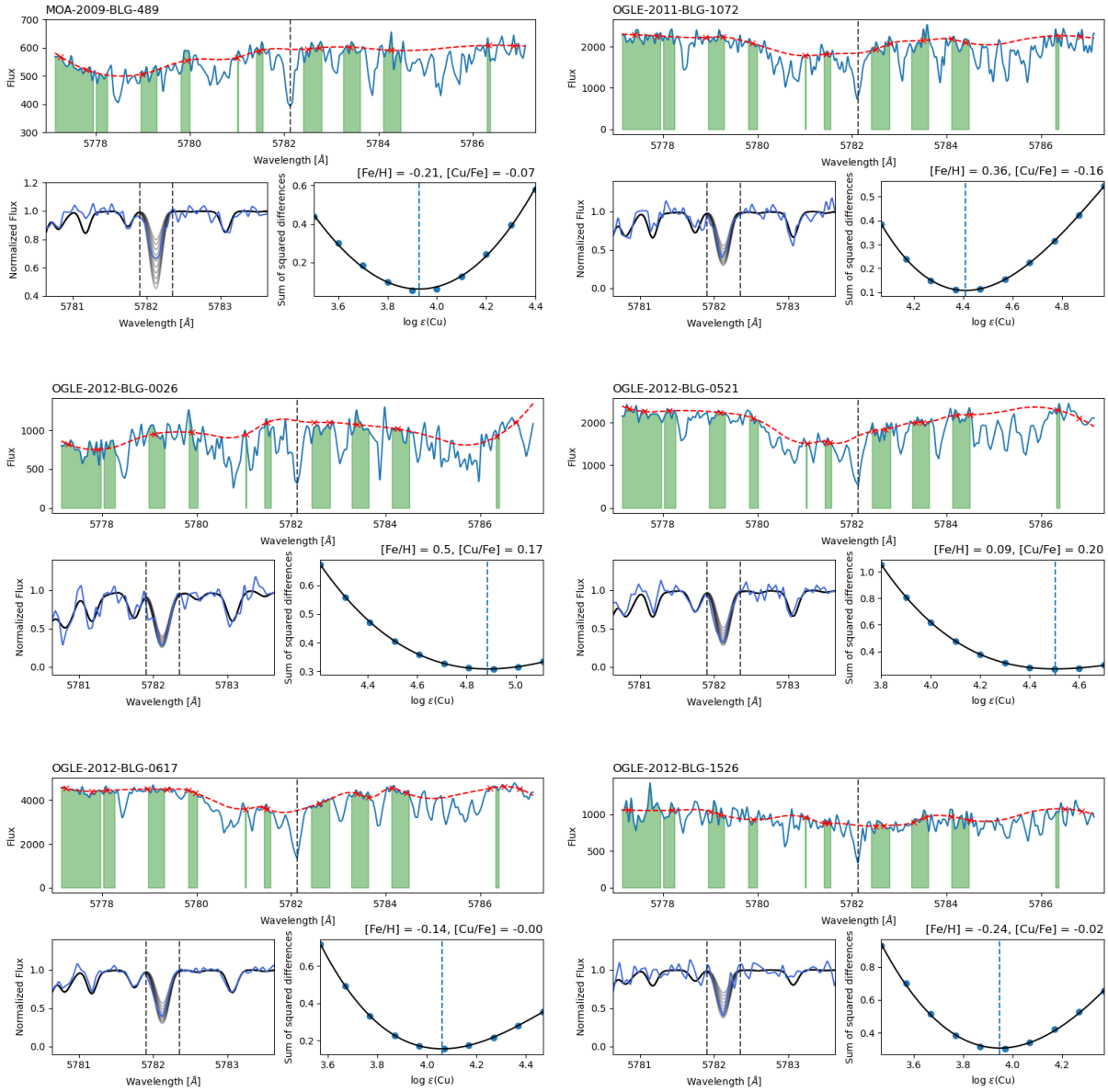

Figure A.3: Same as in Fig. A.1.

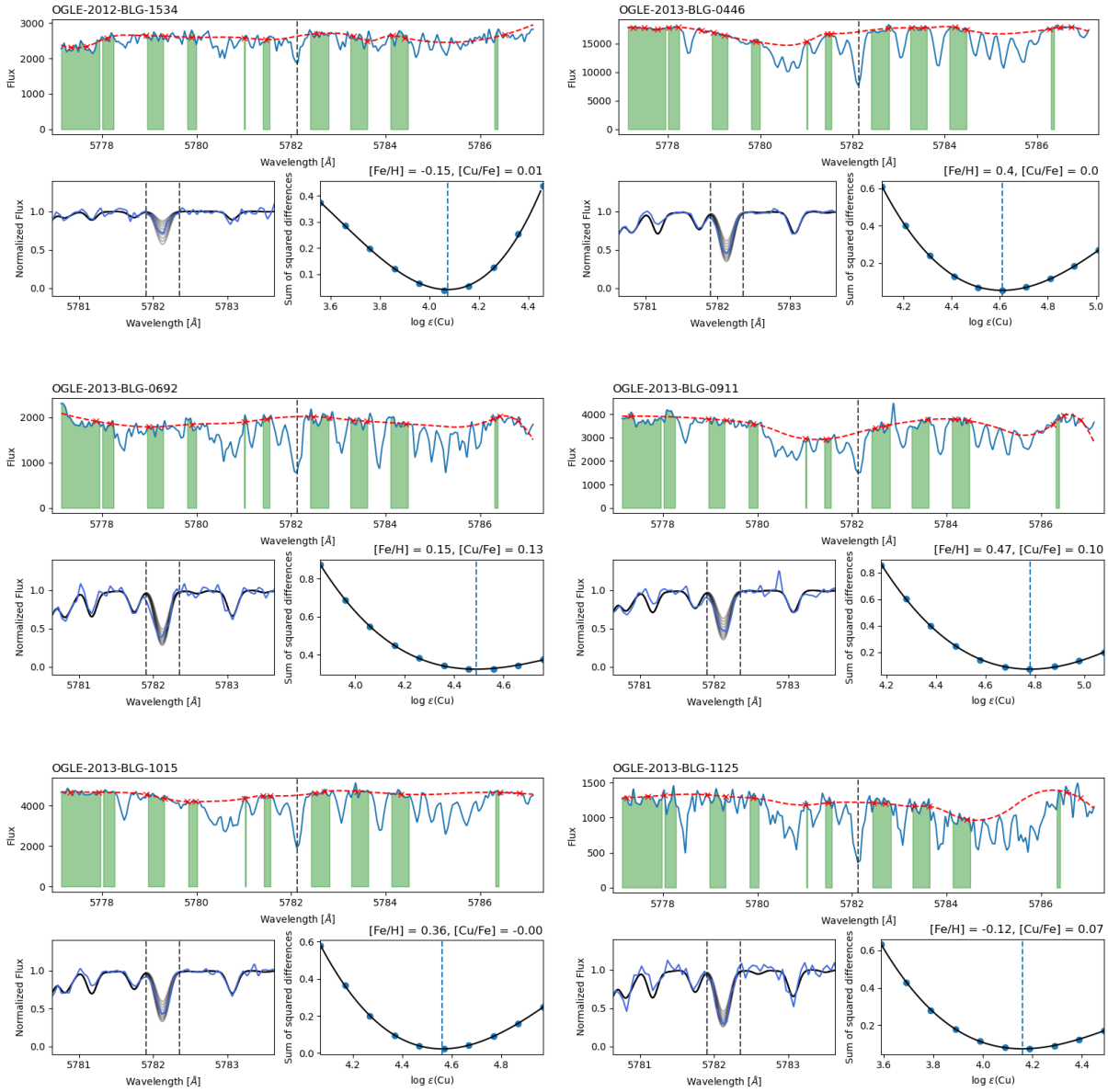

Figure A.4: Same as in Fig. A.1.

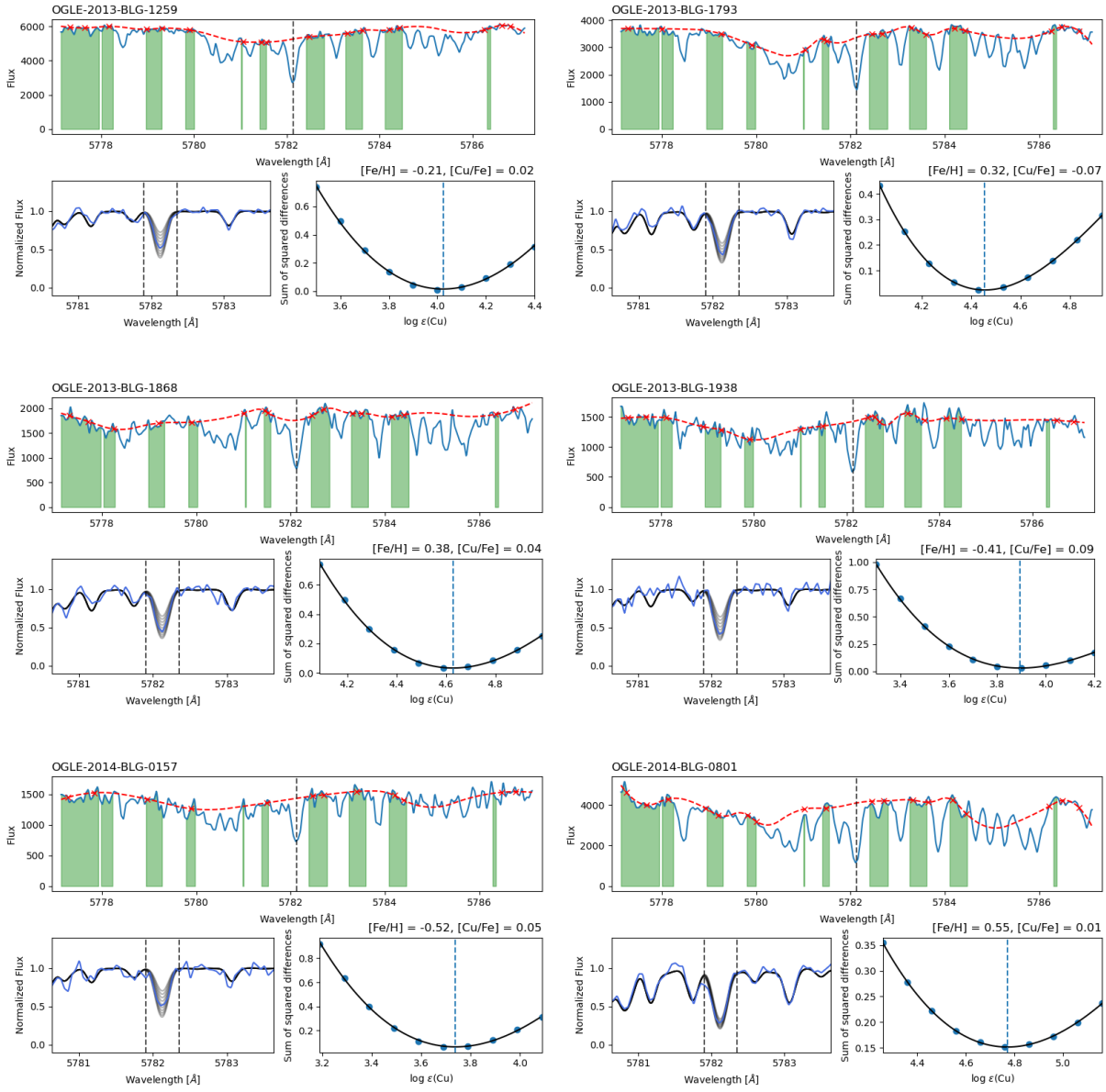

Figure A.5: Same as in Fig. A.1.

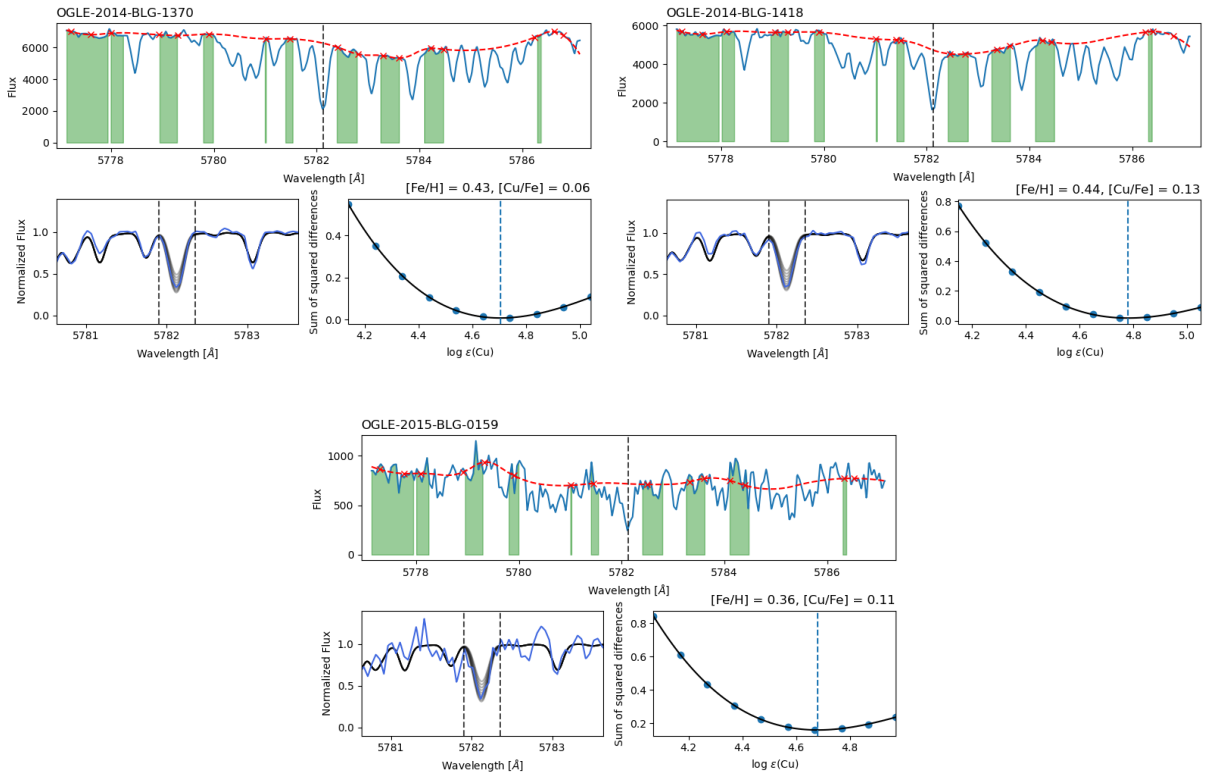

Figure A.6: Same as in Fig. A.1.

A.2 Spectra removed from the final results

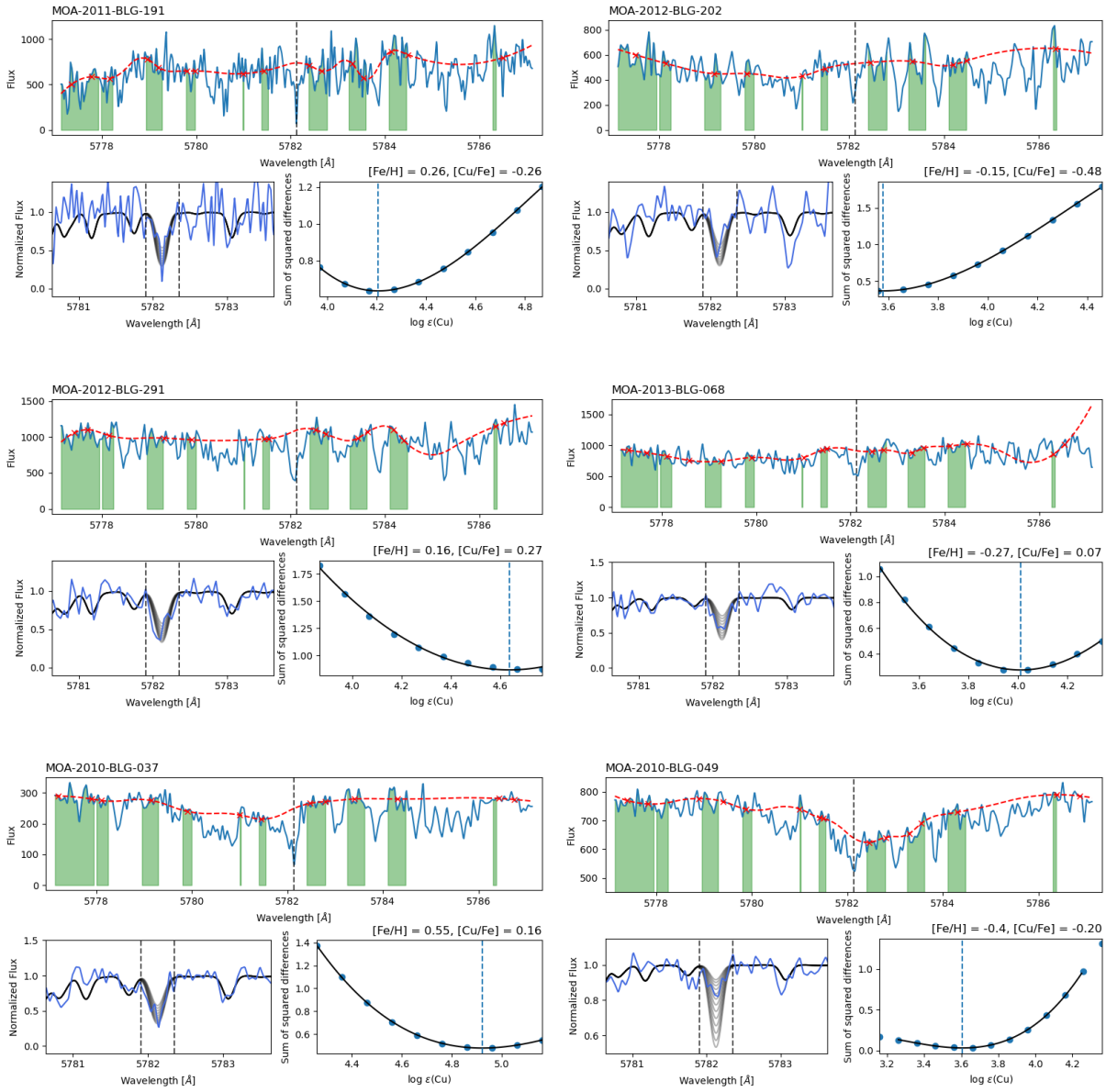

Figure A.7: Similar as to Fig. A.1, these spectra were analysed and a Cu abundance was measured, but where eventually removed from the final results (see Sect. 4.2), due to the Cu spectral line at 5782 Å being disrupted by flux peak(s), causing uncertainty to the Cu abundance measured for the spectrum.

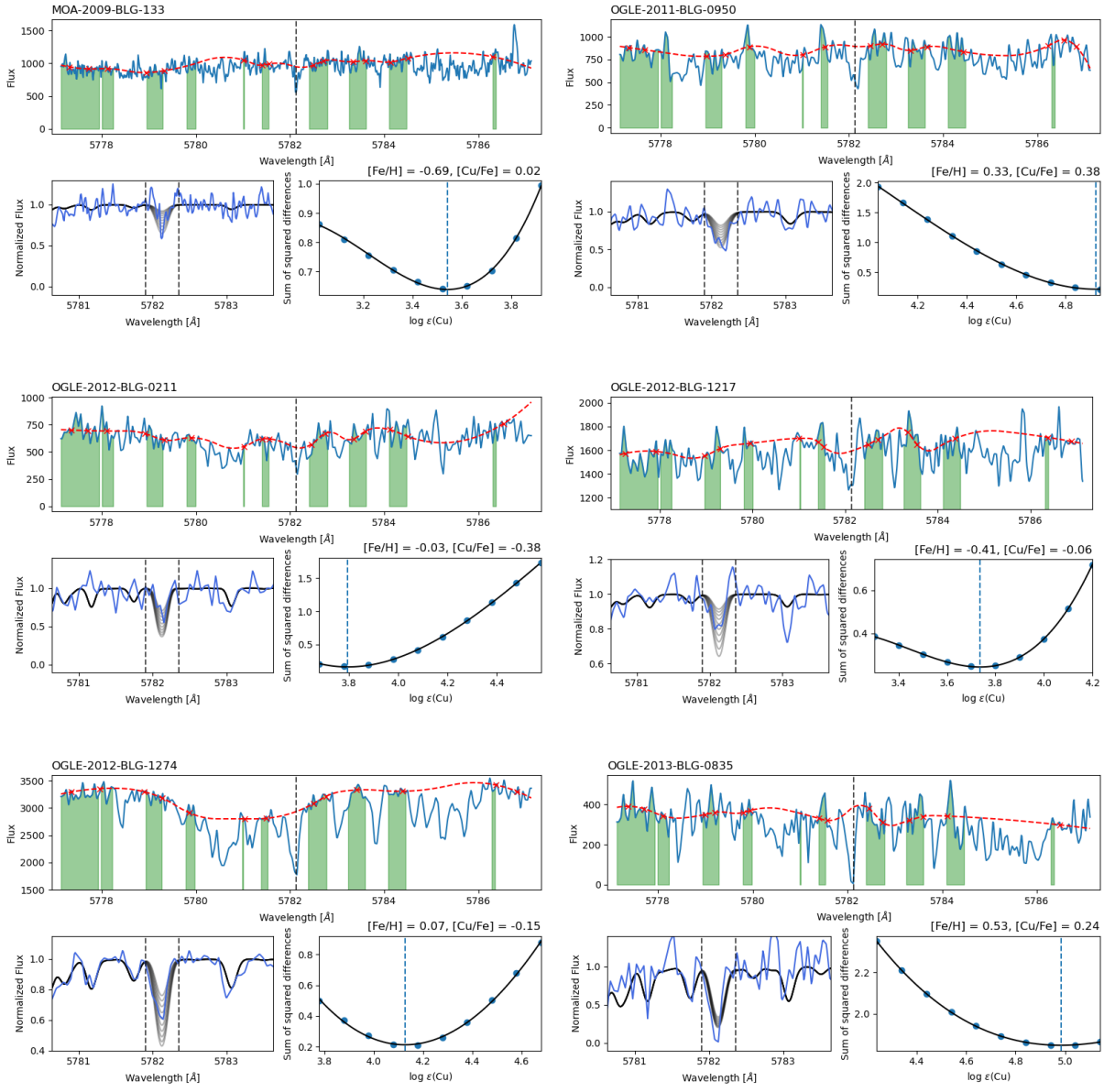

Figure A.8: Same as in Fig. A.7.

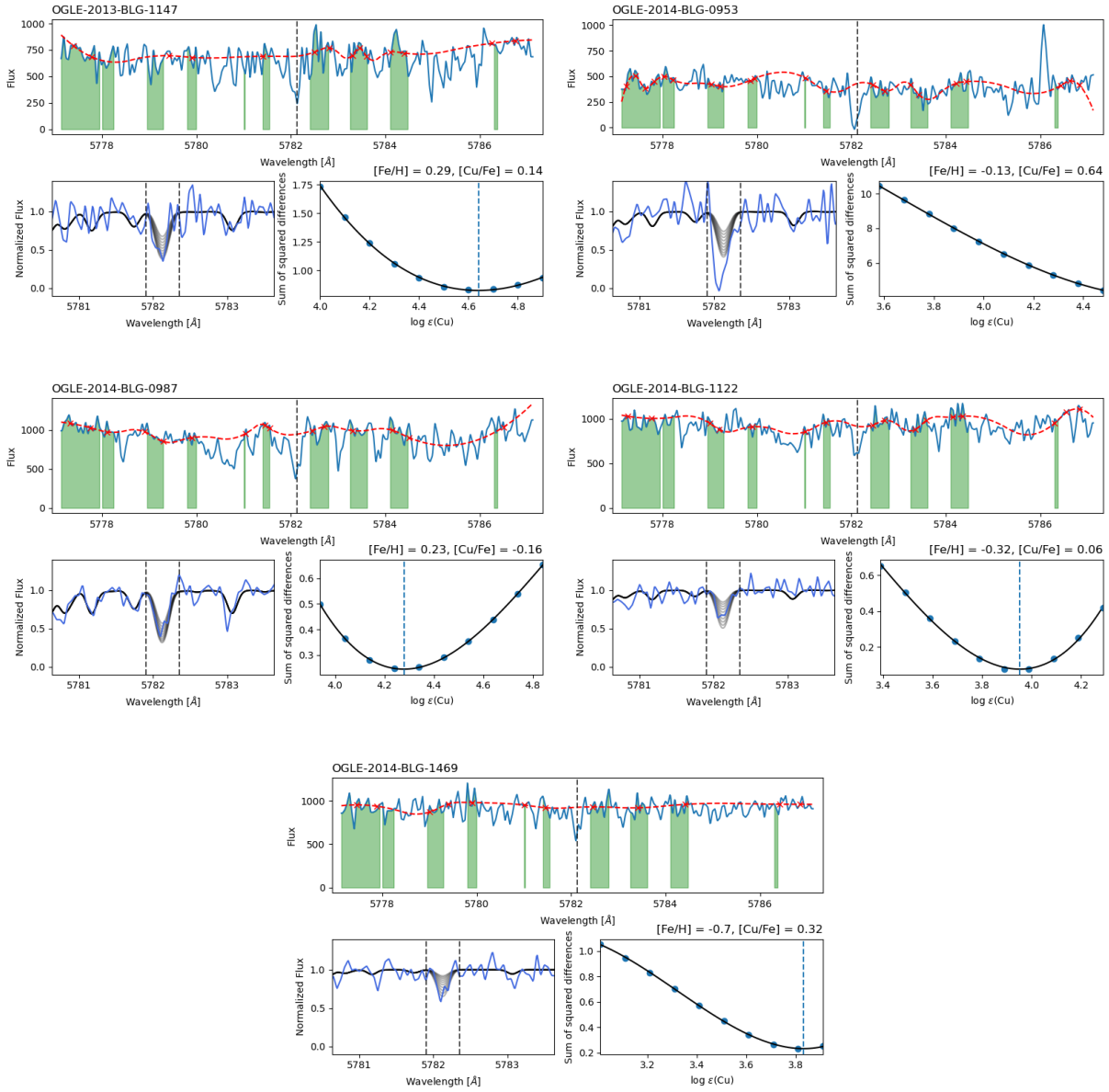

Figure A.9: Same as in Fig. A.7, except for the top-right analysed spectra, which was regarded as an outlier.

A.3 Spectra that could not be analysed for their Cu abundances

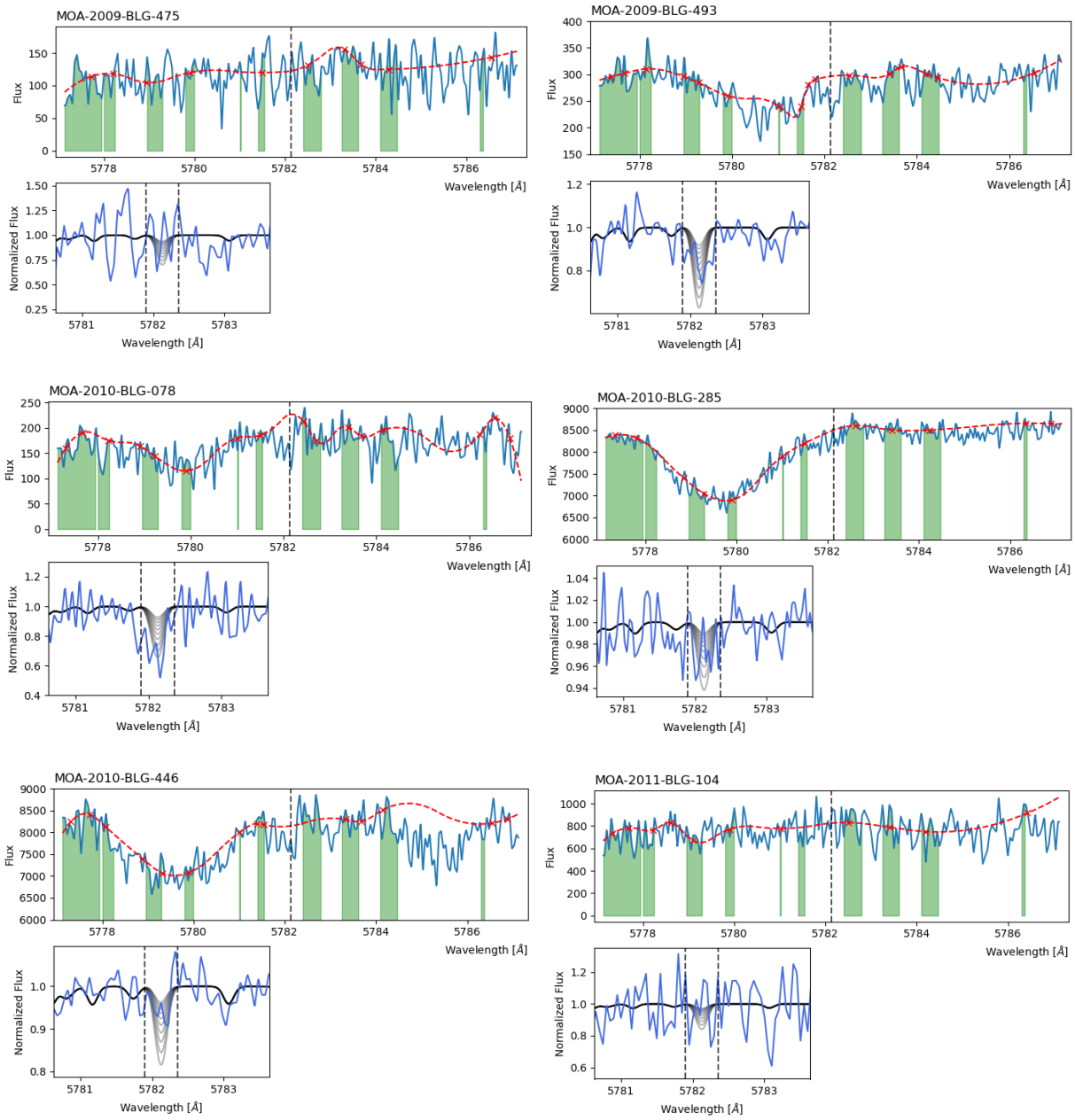

Figure A.10: Same as in Fig. A.1, but the Cu abundance for these spectra were not measured from the Cu spectral line at 5782 Å.

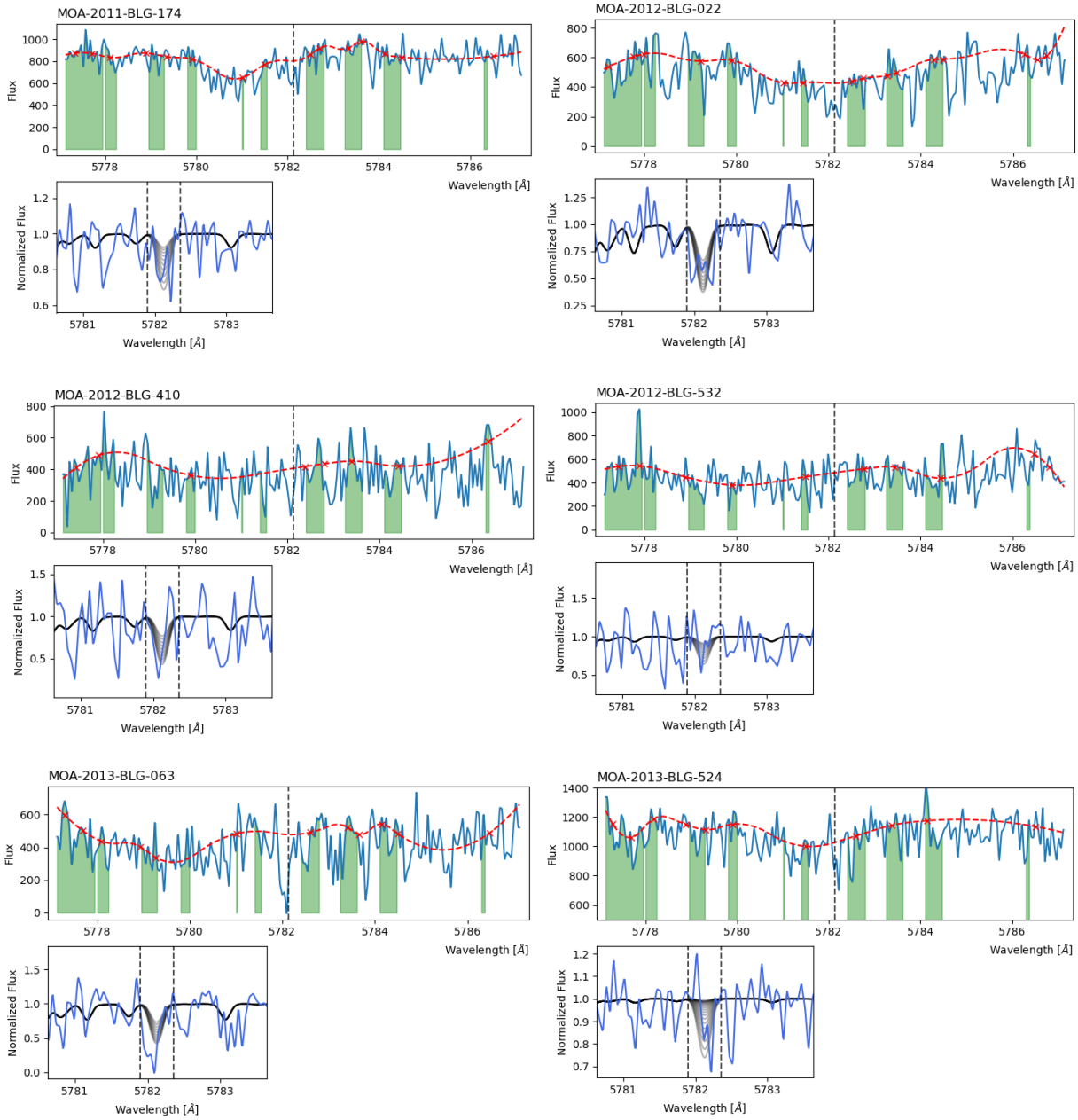

Figure A.11: Same as in Fig. A.10.

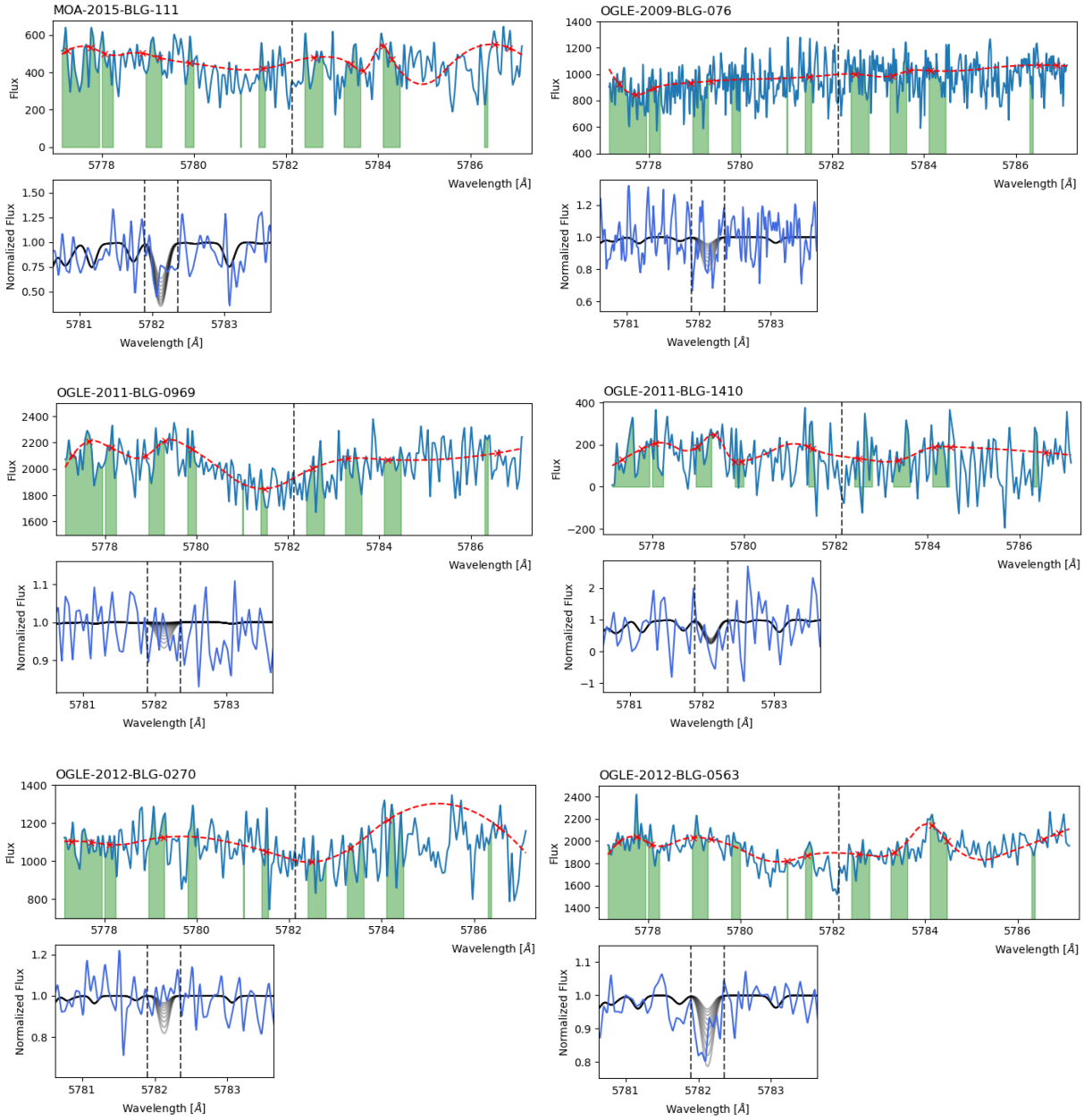

Figure A.12: Same as in Fig. A.10.

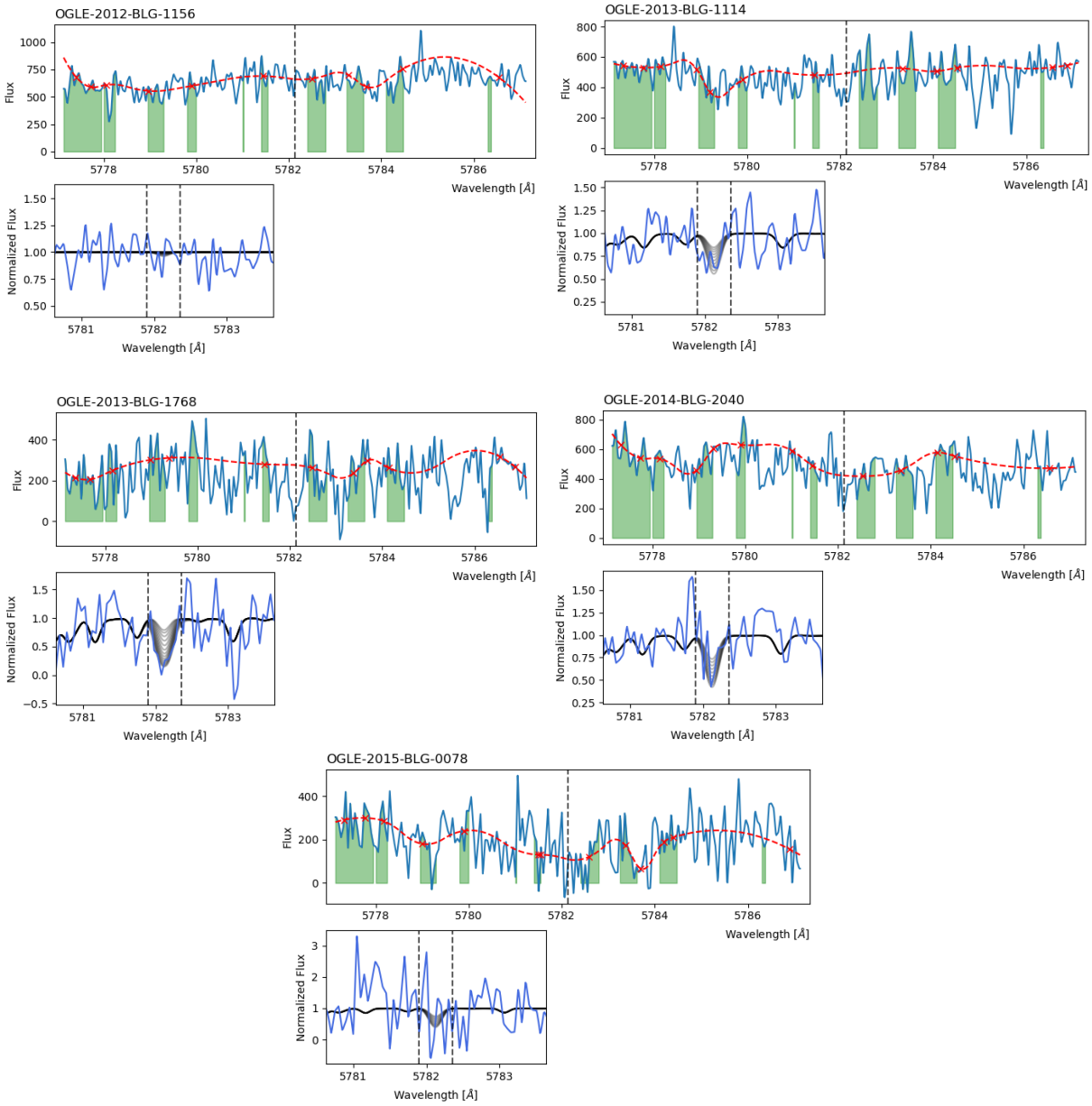

Figure A.13: Same as in Fig. A.10.